

# Deep crustal anatexis, magma mixing, and the generation of epizonal plutons in the Southern Rocky Mountains, Colorado

Kristin H. Jacob · G. Lang Farmer ·  
Robert Buchwaldt · Samuel A. Bowring

Received: 10 June 2014 / Accepted: 5 December 2014  
© Springer-Verlag Berlin Heidelberg 2015

**Abstract** The Never Summer Mountains in north-central Colorado, USA, are cored by two Oligocene, epizonal granitic plutons originally emplaced in the shallow levels of a short-lived (~1 m.y.), small-volume continental magmatic system. The younger Mt. Cumulus stock ( $28.015 \pm 0.012$  Ma) is a syenogranite equivalent compositionally to topaz rhyolites. A comparison to the chemical and isotopic composition of crustal xenoliths entrained in nearby Devonian kimberlites demonstrates that the silicic melts parental to the stock were likely derived from anatexis of local Paleoproterozoic, garnet-absent, mafic lower continental crust. In contrast, the older Mt. Richthofen stock is compositionally heterogeneous and ranges from monzodiorite to monzogranite. Major and trace element abundances and Sr, Nd and Pb isotopic ratios in this stock vary regularly with increasing whole rock wt% SiO<sub>2</sub>. These data suggest that the Mt. Richthofen stock was constructed from mixed mafic and felsic magmas, the former corresponding to lithosphere-derived basaltic magmas similar isotopically to mafic enclaves entrained in the eastern portions of the stock and the latter corresponding to less

differentiated versions of the silicic melts parental to the Mt. Cumulus stock. Zircon U–Pb geochronology further reveals that the Mt. Richthofen stock was incrementally emplaced over a time interval from at least  $28.975 \pm 0.020$  to  $28.742 \pm 0.053$  Ma. Magma mixing could have occurred either *in situ* in the upper crust during basaltic underplating and remelting of an antecedent, incrementally emplaced, silicic intrusive body, or at depth in the lower crust prior to periodic magma ascent and emplacement in the shallow crust. Overall, the two stocks demonstrate that magmatism associated with the Never Summer igneous complex was fundamentally bimodal in composition. Highly silicic anatectic melts of the mafic lower crust and basaltic, mantle-derived magmas were the primary melts in the magma system, with mixing of the two producing intermediate composition magmas such as those from which Mt. Richthofen stock was constructed.

**Keywords** Magma mixing · Topaz rhyolite · Mafic underplating · Crustal anatexis

---

Communicated by Timothy L. Grove.

**Electronic supplementary material** The online version of this article (doi:[10.1007/s00410-014-1094-3](https://doi.org/10.1007/s00410-014-1094-3)) contains supplementary material, which is available to authorized users.

---

K. H. Jacob (✉) · G. L. Farmer  
Department of Geological Sciences, CIRES,  
University of Colorado, Boulder, CO 80309, USA  
e-mail: halbergk@cs.com

R. Buchwaldt · S. A. Bowring  
Department of Earth, Atmospheric, and Planetary Sciences,  
Massachusetts Institute of Technology, Cambridge,  
MA 02139, USA

## Introduction

In many continental magmatic systems, a complex interplay likely exists between mafic magmas injected into the crust from below, melts derived from crustal anatexis, and the crystallized products of both melt compositions, with this interplay varying in style with time, crustal depth, magma volume, and the overall heat budget of the system (McBirney et al. 1987; Wiebe et al. 2002; Acosta-Vigil et al. 2010). Geochronological, chemical, and field studies of exposed continental igneous rocks are generally the only viable options for unraveling the plumbing and compositional evolution of melts in such magmatic systems.

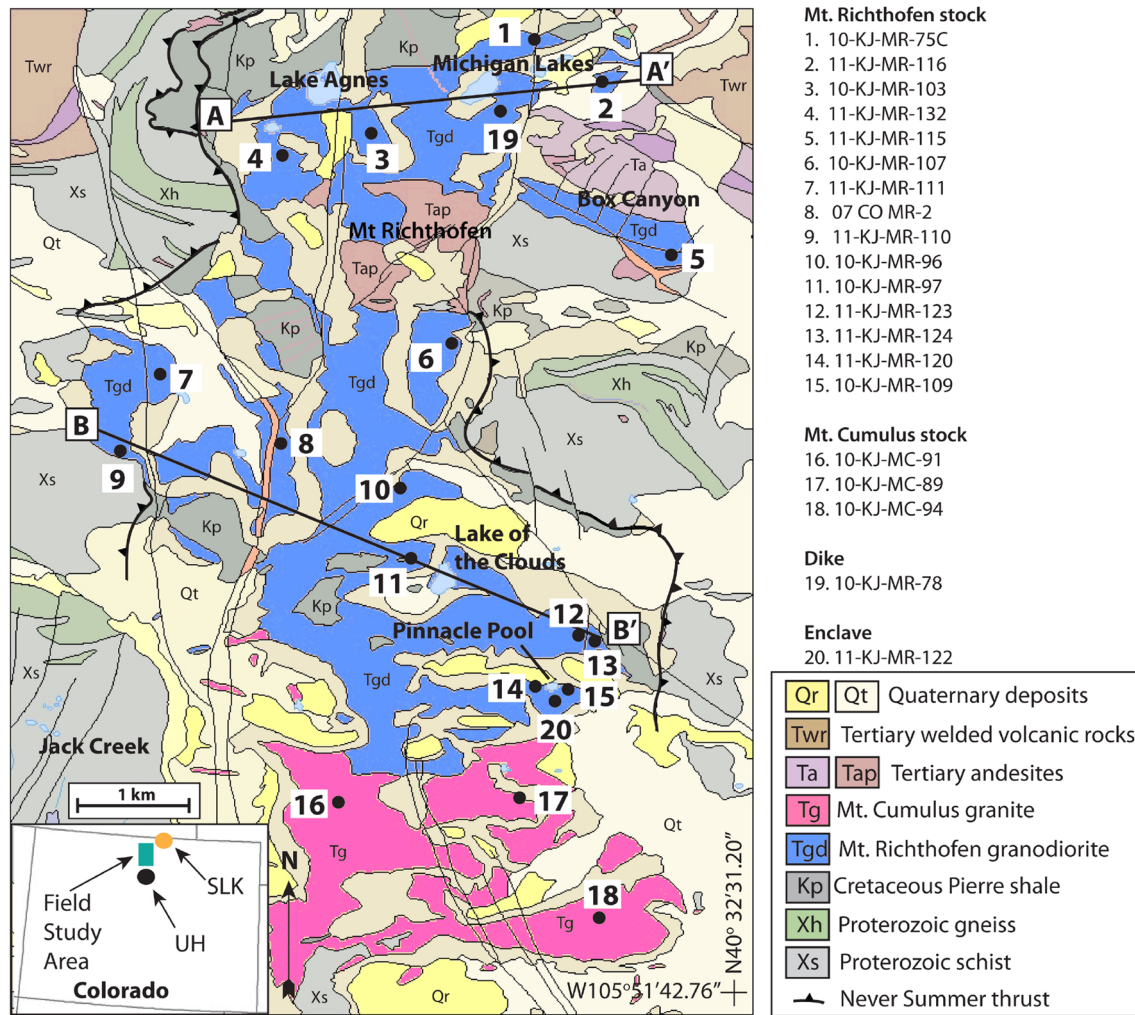


**Fig. 1** Geological map of the intrusive rocks of the Never Summer igneous complex (modified from O'Neill 1981) showing sample localities. Normal faults represented by thin black lines. SLK State Line kimberlite diatremes, UH Urad–Henderson Climax–Mo deposit

However, volcanic rocks only provide information on magmas that breach the surface at the uppermost levels of a given magmatic system. Intrusive igneous rocks, in contrast, may represent complex products of magma input, recharge, and remobilization over a protracted time period and over a restricted range of crustal depths (Harper et al. 2004; Claiborne et al. 2006). Piecing together incomplete information gathered from accessible igneous rocks into a coherent picture of the temporal evolution of a given magma system over its entire spatial extent within the crust is challenging, particularly for large-volume systems that involve multiple, spatially overlapping magmatic episodes.

In this investigation, we explore the possibility that small-volume continental magma systems afford an opportunity to study fundamental aspects of magmatic evolution that may be masked in larger volume systems. For this purpose, we undertook a geochronologic, chemical, and Nd, Sr and Pb isotopic study of two small (~45 km<sup>2</sup> exposed area)

epizonal, Mid-Cenozoic intrusive igneous bodies exposed along the crest of the Never Summer Mountains in north-central Colorado (Fig. 1). The younger Mt. Cumulus stock is a porphyritic syenogranite that intrudes the more heterogeneous Mt. Richthofen stock, the latter varying compositionally from monzodiorite to monzogranite. We argue that because of the small magmatic volumes likely delivered to the upper crust during the history of this igneous center, the intrusive rocks retain decipherable evidence regarding their origin. Our data demonstrate that the magmatism parental to these intrusive rocks was bimodal. Silicic, anatetic melts of mafic, lower continental crust were delivered to the upper crust and solidified as syenogranites such as the Mt. Cumulus stock. Interaction between such silicic melts and mafic, mantle-derived magmas, either at depth or in situ in the shallow crust, led to the more intermediate composition magmas from which the Mt. Richthofen stock was constructed.

## Geologic background

The Oligocene Never Summer igneous complex (also referred to as the Braddock Peak Volcanic Field; Cole et al. 2008; Cole and Braddock 2009) is exposed in north-central Colorado along the western boundary of Rocky Mountain National Park. The complex consists of ~30 km<sup>3</sup> of preserved mafic to silicic composition volcanic rocks (Knox 2005) and two epizonal stocks exposed over ~45 km<sup>2</sup> in the northern half of the Never Summer Mountains (Fig. 1). Volcanic activity commenced at ~29.6 Ma with the deposition of mafic to intermediate lava flows, debris flows, and rhyolites and culminated only ~1.5 m.y. later with the eruption of larger volume topaz rhyolites (Christiansen et al. 1983; Knox 2005). The progression from early intermediate composition volcanism to later silicic ignimbrite deposition is similar to that observed through multiple cycles in the southern Rocky Mountain volcanic field in southern Colorado (Lipman 2007). The latter is generally considered to be the easternmost expression of the mid-Tertiary “ignimbrite flareup”, a period of intense magmatic activity, primarily centered in the western USA, that took place ~25 to 40 Ma (Coney and Reynolds 1977; Armstrong and Ward 1991). The Never Summer igneous complex could represent a significantly smaller and shorter-lived manifestation of this same event. However, the complex is also roughly coincident in time and space with the development of the northernmost Rio Grande rift system in Colorado (Kellogg 1999). Small-volume granite porphyries associated with Climax-style porphyry molybdenum deposits and topaz rhyolites that occur in the late stages of Oligocene magmatism elsewhere in Colorado are likely related to lithospheric extension associated with the Rio Grande rift (Christiansen et al. 2007; Ludington and Plumlee 2009), and this setting may also be relevant for the formation of the Never Summer igneous complex.

Our concern in this study is the origin of the epizonal stocks exposed in the Never Summer Mountains which consist of the intermediate composition Mt. Richthofen stock and the Mt. Cumulus stock syenogranite (O’Neill 1976; Fig. 1). The two stocks, along with common late-stage silicic dikes, represent the bulk of the exposed intrusive rocks in the Never Summer igneous complex. Drill cores reveal that granitic rocks, similar in composition to the Mt. Cumulus stock, also exist beneath the Jack Creek area directly to the west of the Never Summer Mountains (Fig. 1), where they extend to depths of at least 1 km below the present-day surface.

Field relationships demonstrate that the Mt. Richthofen stock shares an intrusive contact with a porphyritic andesite in the area of Mt. Richthofen proper and intrudes into early erupted andesites in the area of Box Canyon along the stock’s eastern margin (Fig. 1). These observations imply a

near surface level of emplacement for this stock. No modern geochronology exists for the Mt. Richthofen stock, but low precision zircon fission track age determinations suggest that the Mt. Richthofen stock is ~28 ± 1 Ma (Gamble 1979), an age that overlaps the range of Ar–Ar ages determined for the intermediate to silicic volcanic rocks at this center (Knox 2005). The Mt. Cumulus stock intrudes the Mt. Richthofen stock along its southernmost margin and so is clearly the younger of the two stocks, although no absolute age determinations for Mt. Cumulus stock exist. The Mt. Cumulus stock must also have been shallowly emplaced, a conclusion consistent with the fact that portions of the stock contain abundant miarolitic cavities (Gamble 1979). Both stocks intrude Precambrian basement rocks and Paleozoic sedimentary rocks along the Late Cretaceous-Early Tertiary Never Summer thrust fault (Fig. 1), a “back thrust” presumably active during the Laramide orogeny and associated with the basement-cored uplift that produced the Colorado Front Range (O’Neill 1976, 1981). Post-intrusion, N–S oriented normal faults, possibly related to extension associated with the Rio Grande rift, cut both stocks although total offset on these faults is unknown (O’Neill 1976). Exhumation of the stocks may have been initiated by this young extensional tectonism but was accelerated by Late Cenozoic glaciation that resulted in the extensive present-day exposures of the stocks along the crest of the Never Summer Mountains.

## Samples and analytical techniques

The basic objective of the study was to use field, petrographic, mineral and whole rock chemical data, U–Pb zircon geochronology, and whole rock Nd, Sr and Pb isotopic analyses to assess the origin of these plutonic rocks and to define the compositions of melts and magmas that were delivered to the upper continental crust during the Oligocene igneous activity. We collected intrusive rock samples across accessible portions of complex at ~1 km intervals. These include fifteen samples of the Mt. Richthofen stock, three samples of the Mt. Cumulus stock, and one sample of a late-stage silicic dike. Three samples of the unexposed syenogranite beneath the Jack Creek area (Fig. 1) were obtained from drill cores available at the USGS Core Research Center in Lakewood, Colorado. During our field investigations, a swarm of mafic enclaves was identified in the southeastern portions of Mt. Richthofen stock, around Pinnacle Pool (Fig. 1). These enclaves are rounded to irregular in shape and are up to 30 cm in length (Fig. 2), and one such enclave was also included in our study.

Whole rock major and trace element data were obtained for all of the samples collected by ICP-MS at Activation Laboratories (Ontario, Canada; Tables 1, 2).



**Fig. 2** Photograph of irregular shaped mafic enclave in host granodiorite collected from the Pinnacle Pool area of the Mt. Richthofen stock (Fig. 1)

Major mineral phase (feldspar and hornblende) compositions were obtained using a JEOL-8600 electron microprobe at the University of Colorado (see Supplementary Information).

Zircons from three samples of the Mt. Richthofen stock and one sample of the Mt. Cumulus stock were extracted for high precision U–Pb age determinations using the CA-TIMS method. Zircon was separated at the Massachusetts Institute of Technology (MIT) using conventional heavy liquid techniques. Uranium and Pb isotopic data were obtained using a VG Sector 54 and IsotopX X-62 mass spectrometers at MIT using analytical procedures from Burgess et al. (2013). Whole rock Nd, Sr and Pb isotopic data from these samples were obtained at the University of Colorado, Boulder using analytical procedures outlined by Farmer et al. (1991). In the following text, all initial isotopic ratios are calculated at 28 Ma.

## Results

### The Mt. Cumulus stock and other highly silicic intrusive rocks

Samples of the Mt. Cumulus stock and Jack Creek (Fig. 1) drill cores are equigranular to porphyritic syenogranites (Streckeisen 1978) with an average mineral mode of 43 % quartz, 9 % plagioclase, 42 % alkali feldspar, 5 % biotite, and <1 % opaque and accessory phases (see supplementary

material for individual sample descriptions). Phenocrysts are generally subrounded anhedral to euhedral and vary in size from 0.5 to 6.0 mm in diameter. Matrix grains are mostly anhedral and range in from 0.01 to 0.2 mm in diameter (Fig. 3). Accessory phases in the Mt. Cumulus stock, identified by Gamble (1979), include zircon, fluorite, and topaz, with less common allanite, apatite, and pyrite. The silicic dike sample contains rounded quartz phenocryst “eyes”, 1–4 mm in length, set in a fine-grained quartz-alkali feldspar matrix. No mafic or accessory minerals were identified in thin section (Fig. 3).

All of the silicic intrusive rock samples have similar bulk compositions, characterized by wt% SiO<sub>2</sub> ranging only from 76.4 to 77.6 wt% (Table 1; Fig. 4). These rocks have high wt% Na<sub>2</sub>O (3.6–4.2 %) and wt% K<sub>2</sub>O (4.4–4.9 %), low total wt% Fe<sub>2</sub>O<sub>3</sub> (1.0–1.5 %; Table 1; Fig. 4), and qualify as ferroan and alkali calcic in the classification schemes of Frost et al. (2001) and Frost and Frost (2008). The rocks are all weakly peraluminous (ASI = molecular Al/(Ca-1.67P + K+Na) = 0.99–1.08; Table 1).

In terms of trace element abundances, the silicic intrusive rocks are characterized by high Rb (165–385 ppm) and Nb contents (54–136 ppm) (Table 2) and relative depletions in Sr and Ba abundances on normalized trace element plots (Figs. 5, 6). These rocks have “seagull”-shaped rare earth element patterns, marked by large negative Eu anomalies (Fig. 6) similar to those commonly observed for high-silica rhyolites (Glazner et al. 2008).

Measured whole rock <sup>87</sup>Sr/<sup>86</sup>Sr for all of the silicic igneous rocks range from 0.7118 to 0.8365 and generally correlate with <sup>87</sup>Rb/<sup>86</sup>Sr ratios, the latter varying up to values as high as 400. These data do not define a statistically significant isochron but do roughly align along an ~28 Ma reference isochron, the presumed crystallization age for the Mt. Cumulus stock (Fig. 7). Initial <sup>87</sup>Sr/<sup>86</sup>Sr ratios are poorly defined for most of the samples because of their high <sup>87</sup>Rb/<sup>86</sup>Sr and the resulting large absolute errors on these ratios (Table 3); however, the lowest <sup>87</sup>Rb/<sup>86</sup>Sr samples yield initial <sup>87</sup>Sr/<sup>86</sup>Sr ratios of ~0.7097. The silicic intrusive rocks measured <sup>143</sup>Nd/<sup>144</sup>Nd ratios show little variation and do not consistently covary with <sup>147</sup>Sm/<sup>144</sup>Nd (Fig. 8). Initial ε<sub>Nd</sub> values for the silicic rock samples range from –5.0 to –6.2 (Table 3; Fig. 9) and <sup>206</sup>Pb/<sup>204</sup>Pb(T) varies between 18.2 and 18.6, <sup>207</sup>Pb/<sup>204</sup>Pb(T) between 15.50 and 15.58, and <sup>208</sup>Pb/<sup>204</sup>Pb(T) between 38.43 and 38.75 (Fig. 10).

Six of the seven zircon grains analyzed from Mt. Cumulus stock sample 10-KJ-MC-91 yielded approximately concordant U–Pb dates (Fig. 11). The weighted mean <sup>206</sup>Pb/<sup>238</sup>U date of these grains is 28.015 ± 0.012 Ma (2σ) with a mean square of the weighted deviates (MSWD) of 0.54, which we interpret as the best estimate of the crystallization age of the Mt. Cumulus stock.

**Table 1** Whole rock major element analyses of the Mt. Richthofen stock, the Mt. Cumulus stock, and associated rocks

Sample no.	Location	Longitude <sup>a</sup>	latitude	elevation <sup>b</sup>	Age <sup>c</sup>	SiO <sub>2</sub>	Al <sub>2</sub> O <sub>3</sub>	Fe <sub>2</sub> O <sub>3</sub> (T)	MnO	MgO
<i>Mt. Richthofen stock</i>										
10-KJ-MR-75C	N of Michigan Lakes	−105.8832	40.4853	3,534		65.51	15.81	4.77	0.08	1.25
10-KJ-MR-96	N of Lake of the Clouds	−105.8887	40.4424	3,432		63.04	16.46	5.67	0.10	1.73
10-KJ-MR-97	W of Lake of the Clouds	−105.8932	40.4337	3,511		61.20	16.22	6.76	0.09	2.13
10-KJ-MR-103	SE of Lake Agnes	−105.8968	40.4779	3,484	28.874 ± 0.017	64.97	16.26	5.14	0.08	1.19
10-KJ-MR-107	W of Skeleton Canyon	−105.8891	40.4575	3,284		62.98	15.81	5.51	0.08	2.28
10-KJ-MR-109	W of Pinnacle Pool	−105.8793	40.4229	3,412	28.975 ± 0.020	55.71	15.99	8.80	0.15	2.98
10-KJ-MR-110	W of Jack Creek drainage	−105.9220	40.4451	3,451		63.89	16.30	5.29	0.07	1.82
11-KJ-MR-111	W of Jack Creek drainage	−105.9178	40.4513	3,292	28.742 ± 0.053	66.55	15.67	4.32	0.07	1.54
07-CO-MR-2	E of Jack Creek drainage	−105.9079	40.4476	3,298		67.38	15.33	4.06	0.06	1.33
10-KJ-MR-116	E of Michigan Lakes	−105.8763	40.4814	3,409		63.93	16.63	5.20	0.08	1.36
11-KJ-MR-115	S of Box Canyon	−105.8705	40.4657	3,275		61.45	16.51	6.42	0.10	1.87
11-KJ-MR-120	W of Pinnacle Pool	−105.8875	40.4208	3,662		55.41	17.27	8.75	0.10	3.16
11-KJ-MR-123	N of Pinnacle Pool	−105.8813	40.4276	3,659		58.35	17.40	7.33	0.12	2.31
11-KJ-MR-124	N of Pinnacle Pool	−105.8779	40.4268	3,559		54.68	17.80	8.94	0.13	2.91
11-KJ-MR-132	SW of Lake Agnes	−105.9107	40.4761	3,482		61.63	16.45	6.00	0.09	1.91
<i>Enclave</i>										
11-KJ-MR-122	SE of Pinnacle Pool	−105.8823	40.4204			51.96	15.71	11.05	0.17	4.80
<i>Mt. Cumulus stock</i>										
Surface samples										
10-KJ-MC-94	E of Red Mountain	−105.8733	40.3992			77.37	12.55	1.08	0.02	0.02
10-KJ-MC-91	peak of Mt Cumulus	−105.8998	40.4123		28.015 ± 0.012	77.02	12.57	1.01	0.02	0.02
10-KJ-MC-89	W of Mt Cumulus	−105.8853	40.4117			76.36	12.86	1.54	0.01	0.10
Core samples										
10-DC-521-2-912	Jack Creek	−105.9626	40.4018			77.42	12.21	1.32	0.02	0.02
10-DC-521-4-931	Jack Creek	−105.9720	40.3972			77.15	12.59	1.16	0.02	0.03
10-DC-521-4-1597	Jack Creek	−105.9720	40.3972			77.62	12.12	1.36	0.02	0.04
<i>Dike</i>										
10-KJ-MR-78	S of Michigan Lakes	−105.8861	40.4798			77.37	12.37	1.30	0.03	0.04
Sample no.	CaO	Na <sub>2</sub> O	K <sub>2</sub> O	TiO <sub>2</sub>	P <sub>2</sub> O <sub>5</sub>	Total	MALI <sup>d</sup>	ASI	AI	K + Na
<i>Mt. Richthofen stock</i>										
10-KJ-MR-75C	2.70	3.76	4.94	0.87	0.32	99.14	6.00	0.98	0.04	0.113
10-KJ-MR-96	3.62	3.82	3.98	1.14	0.45	100.90	4.18	0.99	0.06	0.104
10-KJ-MR-97	4.25	3.58	3.93	1.29	0.55	100.30	3.26	0.94	0.06	0.099
10-KJ-MR-103	2.46	3.59	5.10	0.87	0.32	98.09	6.23	1.05	0.05	0.112
10-KJ-MR-07	4.15	4.47	3.05	1.27	0.41	99.78	3.36	0.89	0.05	0.104
10-KJ-MR-109	6.49	3.97	2.78	2.26	0.87	98.55	0.26	0.79	0.06	0.094
10-KJ-MR-110	3.46	4.04	3.66	1.08	0.38	99.68	4.23	0.99	0.06	0.104
11-KJ-MR-111	2.98	4.30	3.51	0.80	0.28	99.62	4.82	0.98	0.05	0.107
07-CO-MR-2	2.77	4.13	3.94	0.73	0.27	99.02	5.29	0.97	0.04	0.108
10-KJ-MR-116	2.66	4.18	4.63	0.96	0.36	100.30	6.15	1.02	0.05	0.117
11-KJ-MR-115	3.99	3.44	4.42	1.32	0.47	100.30	3.86	0.96	0.06	0.102
11-KJ-MR-120	5.98	4.07	2.71	1.86	0.70	99.19	0.80	0.88	0.08	0.094
11-KJ-MR-123	4.65	3.89	3.99	1.44	0.52	100.90	3.23	0.94	0.07	0.105
11-KJ-MR-124	5.86	3.94	2.96	1.84	0.94	100.60	1.03	0.93	0.08	0.095
11-KJ-MR-132	4.14	4.40	3.64	1.25	0.48	98.51	3.91	0.91	0.05	0.110

**Table 1** continued

Sample no.	CaO	Na <sub>2</sub> O	K <sub>2</sub> O	TiO <sub>2</sub>	P <sub>2</sub> O <sub>5</sub>	Total	MALI <sup>d</sup>	ASI	AI	K + Na
Enclave										
11-KJ-MR-122	5.79	3.40	3.88	2.52	0.73	99.09	1.49	0.81	0.06	0.096
<i>Mt. Cumulus stock</i>										
Surface samples										
10-KJ-MC-94	0.37	4.08	4.44	0.05	0.02	99.62	8.89	1.03	0.01	0.113
10-KJ-MC-91	0.41	4.15	4.75	0.05	0.00	99.07	9.30	0.99	0.01	0.117
10-KJ-MC-89	0.41	3.61	4.88	0.19	0.04	100.20	8.91	1.08	0.02	0.110
Core samples										
10-DC-521-2-912	0.63	3.74	4.56	0.06	0.02	99.08	8.93	1.00	0.01	0.109
10-DC-521-4-931	0.53	3.99	4.47	0.04	0.00	98.63	9.00	1.02	0.01	0.112
10-DC-521-4-1597	0.52	3.75	4.49	0.06	0.01	100.10	8.76	1.01	0.01	0.108
<i>Dike</i>										
10-KJ-MR-78	0.38	3.61	4.83	0.08	0.00	98.74	8.81	1.04	0.01	0.109

Chemical analyses were done by ICP-MS analyses at Activation Laboratories, Canada. All oxide percentages renormalized to 100 % (anhydrous)

Actual analyses totals reported. Total iron reported as Fe<sub>2</sub>O<sub>3</sub>

<sup>a</sup> Sample locations given in decimal degrees

<sup>b</sup> Elevation given in meters

<sup>c</sup> Ages are in m.y. and represent U–Pb zircon analyses done by TIMS at MIT, Cambridge, MA

<sup>d</sup> Classifications based on Frost et al. (2001). MALI modified alkali lime index, ASI aluminum saturation index, AI alkalinity index; K + Na reported on a molecular basis

## Mt. Richthofen stock

### Petrography, major, and trace element compositions

Unlike the relatively uniform bulk compositions of the syenogranites, the Mt. Richthofen stock spans a wide compositional range from monzodiorite to monzogranite. The more mafic lithologies comprise the eastern portions of the stock, and more felsic lithologies are found to the west. Mafic minerals include biotite, hornblende and, in more mafic samples, clinopyroxene (Fig. 3). Accessory mineral assemblages include ubiquitous apatite and oxide minerals. Allanite and zircon occur in the more felsic samples, while titanite is restricted to more mafic rocks (see supplementary material for individual sample descriptions).

Weight% SiO<sub>2</sub> values vary in the Mt. Richthofen stock from 54 % in the east to 67 % in the west (Table 1). Wt% CaO, Fe<sub>2</sub>O<sub>3</sub> (T), Al<sub>2</sub>O<sub>3</sub>, P<sub>2</sub>O<sub>5</sub>, and TiO<sub>2</sub> co-vary with wt% SiO<sub>2</sub>, while both wt% Na<sub>2</sub>O and wt% K<sub>2</sub>O average ~4 wt%, regardless of silica content (Fig. 4). Strontium, Ba, and Sc concentrations generally decrease, and Th and U generally increase, with increasing wt% SiO<sub>2</sub> (Table 2; Fig. 5). Overall, the stock is light rare element (LREE) enriched and REE abundances decrease with increasing wt% SiO<sub>2</sub> from east to west across the stock. Trace element patterns are smooth and display only minor negative Nb anomalies and no Ta anomaly (Fig. 6).

The mafic enclave has major and trace element compositions that fall near the lower wt% SiO<sub>2</sub> extensions of linear

regression curves fitted to the Mt. Richthofen stock compositions on Harker and trace element variation diagrams (Figs. 4, 5). The enclave is LREE enriched, contains REE concentrations comparable to most mafic samples of the Mt. Richthofen stock, and displays a minor negative Eu anomaly (Eu/Eu\* ~ 0.79) but no negative Nb or Ta anomalies on a normalized trace element plot (Fig. 6).

### Mineral thermometry/barometry

Feldspar and amphibole compositions in the most mafic, easternmost portions of the Mt. Richthofen stock near Pinnacle Pool (Fig. 1) were measured to estimate final mineral equilibration pressures and temperatures. Plagioclase compositions from these rocks fall in the range of An<sub>34–55</sub> (Supplementary Material). Alkali feldspar is mainly orthoclase with an albite component around 17.6 mol%. Amphiboles are generally calcic (edenite; Leake 1997) with Mg numbers from 57 to 64 (Supplementary Material). Weight% Al<sub>2</sub>O<sub>3</sub> and wt% TiO<sub>2</sub> range from 4.0 to 6.7 and from 0.13 to 0.96, respectively.

These rocks contain the requisite buffering assemblage (hornblende, biotite, titanite, magnetite, plagioclase, alkali feldspar, quartz), along with clinopyroxene, for the application of Al-in-igneous hornblende geobarometer (Anderson and Smith 1995). Pressure estimates range from 0.5 to 2.7 kbar with an average of 1.0 kbar (100 MPa), and, when combined with the plagioclase-hornblende (Blundy and Holland 1990;

**Table 2** Whole rock trace element analyses of the Mt. Richthofen stock, the Mt. Cumulus stock, and associated rocks

Sample no.	Sc	V	Co	Zn	Ga	Ge	Rb	Sr	Y	Zr	Nb	Sn	Cs	Ba	La	Ce	Pr
<i>Mt. Richthofen stock</i>																	
10-KJ-MR-75C	7	48	7	80	22	1.2	134	516	26.7	308	45.5	2	2.7	1,180	65.3	127	14.4
10-KJ-MR-96	10	70	9	80	22	1.4	110	685	27.2	333	54.5	3	4.4	1,178	62.9	126	14.3
10-KJ-MR-97	11	102	13	70	24	1.5	130	673	30.6	308	49.3	3	5.4	1,125	70.6	140	16.2
10-KJ-MR-103	7	49	8	90	26	2.1	164	330	28.1	364	49.8	4	1.9	1,223	58.5	117	12.3
10-KJ-MR-107	10	93	11	70	20	1.3	78	716	18.5	261	39.5	7	1.3	1,149	65.9	129	14.1
10-KJ-MR-109	12	144	18	110	21	1.3	71	1,025	25.6	385	74.4	7	1.8	1,152	74.8	155	18.0
10-KJ-MR-110	8	81	15	90	23	1.3	92	821	19.7	273	39.2	2	1.9	1,373	60.2	116	12.9
11-KJ-MR-111	7	64	10	60	22	1.2	90	906	14.8	205	28.2	1	1.7	1,433	52.6	98.8	10.8
07-CO-MR-2	6	57	9	50	23	1.1	107	877	15.5	216	29.9	1	3.6	1,469	60.6	109	12.0
11-KJ-MR-115	11	91	12	110	24	1.5	130	622	30.8	382	53.3	4	4.5	1,293	65.7	133	15.4
10-KJ-MR-116	8	50	8	70	24	1.9	140	625	29.5	412	51.4	3	3.1	1,544	63.3	130	15.2
11-KJ-MR-120	14	163	21	90	24	1.4	78	1,046	18.6	393	37.9	12	2.1	1,340	60.1	114	12.4
11-KJ-MR-123	13	103	14	100	26	1.4	125	882	28.2	407	50.5	2	2.7	1,873	54.9	114	14.0
11-KJ-MR-124	11	129	19	120	26	1.3	79	1,067	24.9	217	49.0	2	4.2	1,339	52.6	109	13.3
11-KJ-MR-132	10	84	12	70	24	1.6	112	529	31.3	327	49.9	3	1.1	836	72.9	137	15.6
<i>Enclave</i>																	
11-KJ-MR-122	19	192	25	130	25	1.6	146	652	31.7	301	80.8	27	6.9	1,326	73.1	152	18.3
<i>Mt. Cumulus stock</i>																	
Surface samples																	
10-KJ-MC-94	1	5	1	30	27	2.1	385	4	65.7	140	136	10	6.3	21	29.8	74.5	9.1
10-KJ-MC-91	1	5	1	30	26	2.2	382	3	73.4	137	135	2	9.1	16	41.1	95.9	11.3
10-KJ-MC-89	2	5	1	30	22	1.5	181	83	29.9	195	54	8	2.2	334	64.2	126	13.8
Core samples																	
10-DC-521-2-912			1	50	24	2.1	272		83.0	160	103	8	3.3		31.5	80.8	11.1
10-DC-521-4-931	2	5	1	30	27	2.2	344	4	92.6	148	136	4	6.5	8	27.4	74.4	10.0
10-DC-521-4-1597	2	5	1	40	26	1.8	307	15	81.2	172	134	72	3.2	21	37.2	94	11.8
<i>Dike</i>																	
10-KJ-MR-78	2	5	1	90	23	1.2	165	101	56.0	182	66.1	6	1.3	85	48.4	110	13.2
<i>Reproducibility</i>																	
Percent <sup>a</sup>	6	7	7	23	2		10	15	19	10	4		14	5	7	3	3
Sample no.	Nd	Sm	Eu	Gd	Tb	Dy	Ho	Er	Tm	Yb	Lu	Hf	Ta	Tl	Pb	Th	U
<i>Mt. Richthofen stock</i>																	
10-KJ-MR-75C	52.1	8.99	1.98	6.42	0.95	4.98	0.96	2.6	0.37	2.49	0.41	7.9	3.23	0.54	16	15.3	2.86
10-KJ-MR-96	55.9	10.6	2.22	6.94	1.10	6.08	1.08	2.95	0.41	2.79	0.43	8.5	3.95	0.44	20	15.4	3.43
10-KJ-MR-97	60.1	10.8	2.55	8.12	1.13	6.15	1.09	3.02	0.41	2.65	0.42	7.8	3.29	0.63	25	16.6	3.42
10-KJ-MR-103	45.7	8.33	2.09	5.97	0.91	4.91	0.92	2.63	0.38	2.46	0.37	7.6	4.12	0.80	18	16.9	3.66
10-KJ-MR-107	52.5	8.99	2.03	5.49	0.79	4.30	0.75	1.94	0.26	1.70	0.26	6.4	2.82	0.49	21	12.4	2.76
10-KJ-MR-109	71.6	12.8	2.93	8.16	1.18	6.26	1.07	2.62	0.35	2.21	0.33	8.5	4.49	0.37	14	7.7	1.79
10-KJ-MR-110	46.3	7.83	2.07	5.46	0.73	3.81	0.68	1.8	0.24	1.61	0.25	6.6	2.71	0.40	19	12.8	2.63
11-KJ-MR-111	38.2	6.17	1.58	4.27	0.54	2.79	0.50	1.31	0.19	1.23	0.19	5.2	2.32	0.33	19	15.9	3.45
07-CO-MR-2	41.3	6.62	1.56	4.37	0.54	2.90	0.51	1.38	0.20	1.38	0.22	5.5	2.47	0.54	19	20.7	4.20
11-KJ-MR-115	57.8	10.4	2.48	7.74	1.13	5.94	1.07	2.98	0.42	2.72	0.43	9.1	3.40	0.56	20	15.3	3.68
10-KJ-MR-116	56.0	10.3	2.25	7.30	1.06	5.64	1.01	2.66	0.37	2.40	0.39	9.6	2.97	0.54	16	12.6	2.69
11-KJ-MR-120	46.0	8.02	2.21	6.07	0.79	3.85	0.69	1.87	0.25	1.64	0.25	8.2	2.27	0.45	19	6.9	1.49
11-KJ-MR-123	54.1	10.0	2.76	7.93	1.11	5.81	1.02	2.74	0.38	2.45	0.37	9.0	2.75	0.81	15	10.3	1.35
11-KJ-MR-124	52.6	9.7	2.62	7.02	0.98	5.00	0.92	2.32	0.31	1.98	0.30	5.2	3.06	0.39	15	8.2	1.48
11-KJ-MR-132	58.7	10.5	2.47	7.58	1.10	5.91	1.09	2.97	0.42	2.73	0.43	8.1	3.30	0.47	10	15.6	3.34

**Table 2** continued

Sample no.	Nd	Sm	Eu	Gd	Tb	Dy	Ho	Er	Tm	Yb	Lu	Hf	Ta	Tl	Pb	Th	U
Enclave																	
11-KJ-MR-122	70.1	13.0	2.89	9.49	1.30	6.82	1.20	3.19	0.43	2.72	0.42	6.8	4.20	1.07	14	6.9	1.94
<i>Mt. Cumulus stock</i>																	
Surface samples																	
10-KJ-MC-94	35.9	10.5	0.005	8.77	1.84	12.3	2.42	7.05	1.13	7.93	1.28	8.0	12.40	1.45	20	42.2	4.34
10-KJ-MC-91	41.5	10.9	0.005	8.63	1.83	12.5	2.51	7.58	1.26	9.13	1.45	8.5	15.40	1.14	32	54.6	12.90
10-KJ-MC-89	48.4	9.1	0.43	5.67	0.96	6.1	1.14	3.28	0.51	3.42	0.53	6.6	4.45	0.75	20	26.1	7.95
Core samples																	
10-DC-521-2-912	44.5	14.0	0.034	14.2	2.59	15.7	3.01	8.85	1.34	8.72	1.33	8.3	6.38	0.96	30	31.8	12.2
10-DC-521-4-931	41.1	13.5	0.005	12.0	2.58	17.1	3.36	9.75	1.53	10.7	1.69	9.3	11.80	1.35	26	43.0	17.2
10-DC-521-4-1597	46.8	13.8	0.005	11.4	2.37	15.6	3.05	8.74	1.34	9.39	1.50	10.0	12.20	1.51	30	45.3	10.7
Dike																	
10-KJ-MR-78	48.9	12.0	0.087	10.5	1.84	11.3	2.05	5.83	0.87	5.65	0.87	6.7	4.98	0.95	33	28.1	7.24
Reproducibility																	
Percent <sup>a</sup>	3	2	4	7	1	3	3	5	2	3	3	7	9		17	1	2

Concentrations (ppm) done by ICP-MS at Activation Laboratories, Canada

<sup>a</sup> Estimated external reproducibilities are % of mean standard concentrations based on repeated measurements of blind standard

**Fig. 3** Thin section photomicrographs of rocks from the Mt. Richthofen and Mt. Cumulus stocks and silicic dike. **a** Granodiorite from the most mafic portion of the Mt. Richthofen stock with phenocrysts of plagioclase, biotite and clinopyroxene, and minor oxide minerals. **b** Monzogranite from the most felsic portion of the Mt. Richthofen stock features fine-grained quartz and alkali feldspar (not labeled) surrounding larger plagioclase and biotite phenocrysts. The modal abundance of mafic minerals decreases, and the average grain size increases from plates **a** to **b**. **c** Porphyritic syenogranite from the Mt. Cumulus stock. Quartz crystals are surrounded by a fine-grained quartz-feldspar matrix with minor biotite (not labeled). **d** Silicic dike with rounded quartz phenocrysts set in a fine-grained quartz-alkali feldspar matrix. Abbreviations are as follows: *Qz* quartz, *Pl* plagioclase, *Cpx* clinopyroxene, *Bt* biotite, *Fsp* feldspar

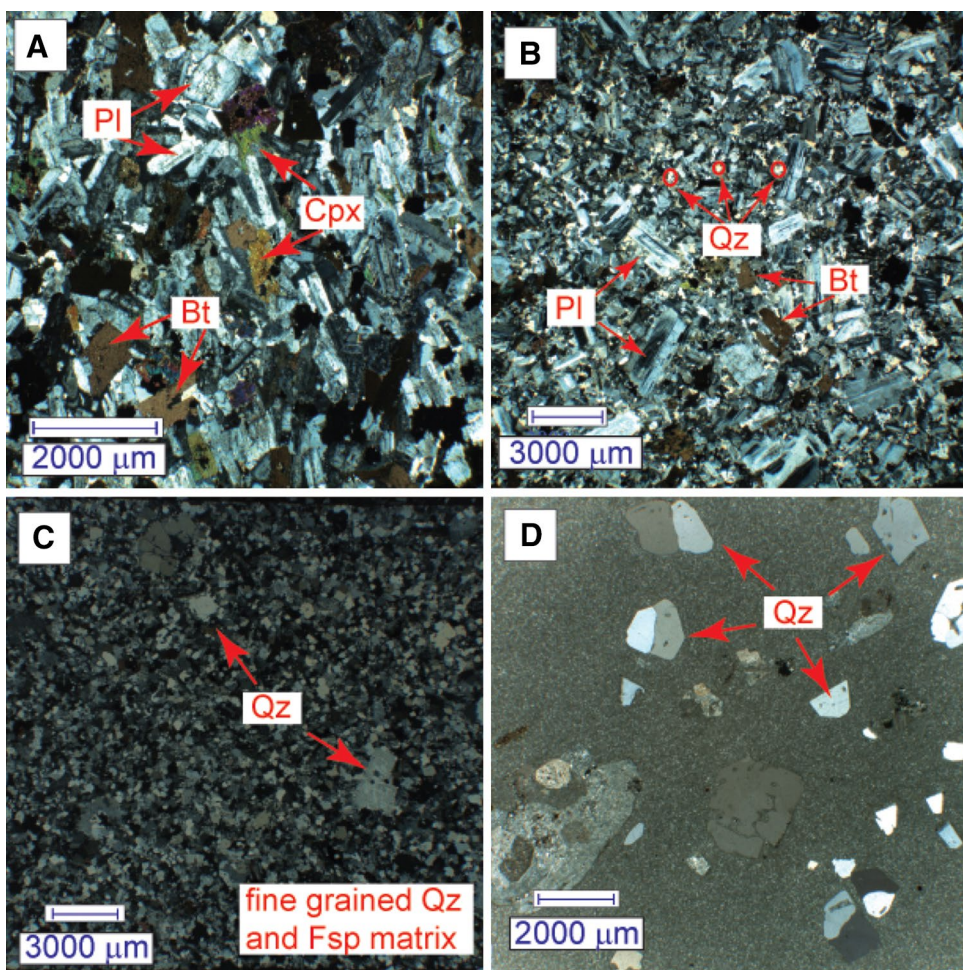
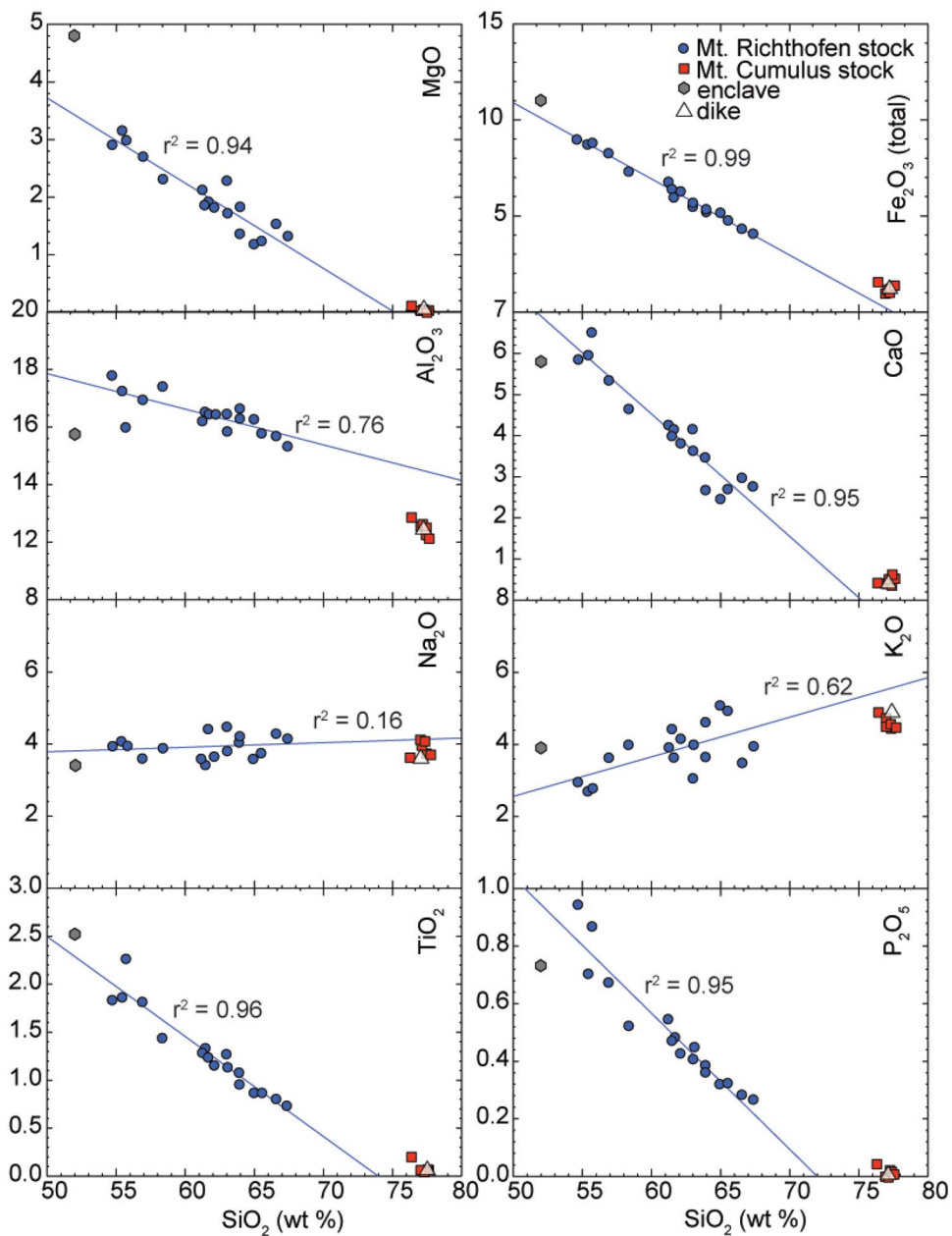


**Fig. 4** Major element Harker variation diagrams for intrusive rock samples from the Never Summer igneous complex. Major element compositions are normalized to volatile-free values. Regression lines are fitted to the Mt. Richthofen stock compositions



Holland and Blundy (1994) and two-feldspar thermometers (Putirka 2008), yield equilibration temperatures of 650–800 °C and 700–780 ± 30 °C, respectively, (Supplementary Material). These temperatures are at or below the granite solidus and so may reflect subsolidus equilibration rather than crystallization temperatures.

#### Whole rock isotopic compositions and zircon U–Pb geochronology

Measured whole rock  $^{87}\text{Sr}/^{86}\text{Sr}$  ratios of the Mt. Richthofen stock range from 0.7049 to 0.7125, independently of  $^{87}\text{Rb}/^{86}\text{Sr}$  ratios. The latter vary over only a narrow range, at values uniformly <2 (Table 3; Fig. 7). Similarly,

measured  $^{143}\text{Nd}/^{144}\text{Nd}$  vary over a considerable range (0.51232–0.51259) despite little variation in whole rocks  $^{147}\text{Sm}/^{144}\text{Nd}$  (Table 3; Fig. 8). Whole rock  $\varepsilon_{\text{Nd}}(\text{T})$  values of the Mt. Richthofen stock range from −0.53 to −5.76 with the more mafic, southern portions of the stock yielding higher  $\varepsilon_{\text{Nd}}(\text{T})$  (−0.53 to −2.45), and the more silicic portions to the west yielding lower values (average −5.58; Fig. 9). Whole rock  $^{206}\text{Pb}/^{204}\text{Pb}(\text{T})$ ,  $^{207}\text{Pb}/^{204}\text{Pb}(\text{T})$ , and  $^{208}\text{Pb}/^{204}\text{Pb}(\text{T})$  generally range from 17.72 to 18.61, 15.45 to 15.58, and 37.50 to 38.64, respectively, with samples from the western portion of the stock yielding less radiogenic initial Pb compositions (Table 3; Fig. 10). Isotopically, the enclave falls within the range of values of the Mt. Richthofen stock.

**Fig. 5** Trace element variation diagrams for intrusive rock samples from the Never Summer igneous complex. Regression lines are fitted to the Mt. Richthofen stock compositions

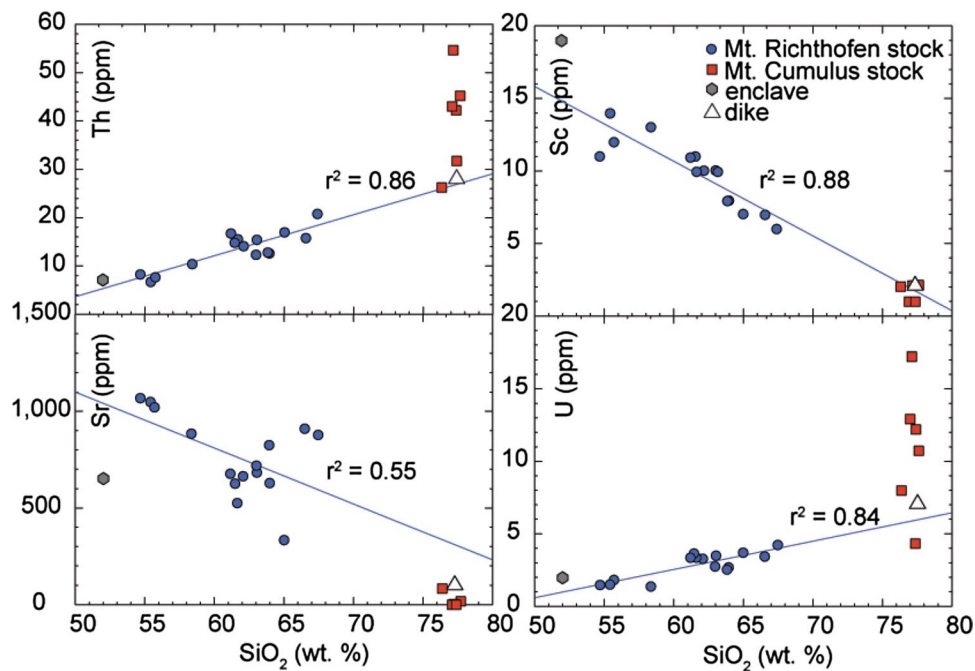
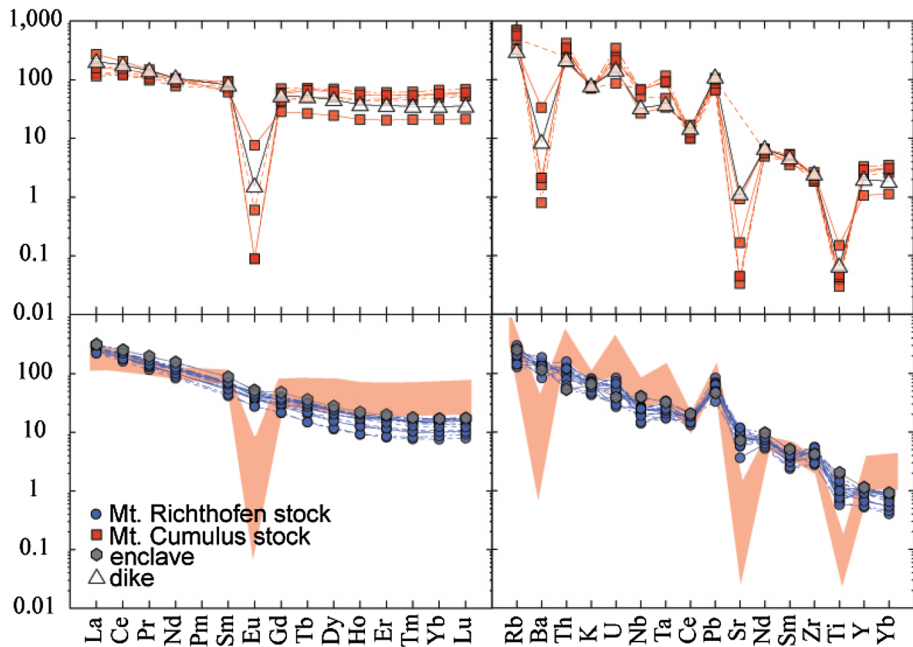


**Fig. 6** Trace element REE and spider diagrams for the intrusive rock samples from the Never Summer igneous complex. Element concentrations normalized to the primitive mantle values of McDonough and Sun (1995)



Eight of ten zircon grains analyzed from sample 10-KJ-MR-103 from the Lake Agnes area (Fig. 1) yielded concordant U–Pb dates with a weighted mean  $^{206}\text{Pb}/^{238}\text{U}$  date of  $28.874 \pm 0.017$  Ma ( $2\sigma$ ) and a MSWD of 0.94 (Fig. 11; Supplementary Material). Six of seven zircon grains from sample 10-KJ-MR-109, from the eastern, more mafic, portions of the stock, yielded concordant U–Pb dates with a weighted mean  $^{206}\text{Pb}/^{238}\text{U}$  date of  $28.975 \pm 0.020$  Ma ( $2\sigma$ ) and a MSWD of 1.1. Finally, four of five zircon grains from sample 11-KJ-MR-111, from the western portion of the stock (Fig. 1)

yielded a concordant  $^{206}\text{Pb}/^{238}\text{U}$  date of  $28.742 \pm 0.053$  Ma ( $2\sigma$ ) and a MSWD of 0.97 (Fig. 11; Supplementary Material).

## Discussion

Our data clearly illustrate that fundamental differences exist between the chemical and isotopic compositions of the two studied stocks. The older Mt. Richthofen stock (28.74 Ma to 28.98 Ma) is chemically and isotopically

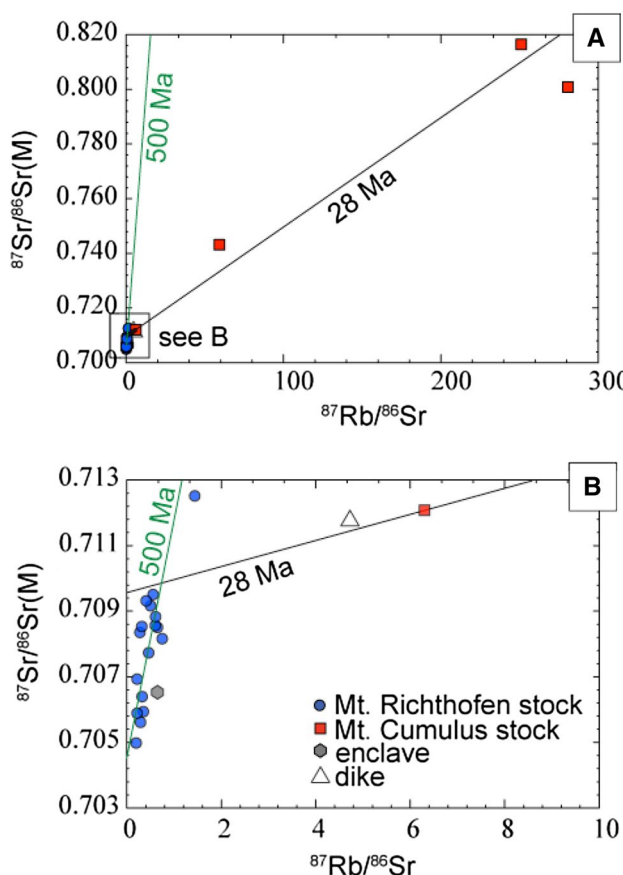


**Fig. 7** Measured  $^{87}\text{Sr}/^{86}\text{Sr}$  versus  $^{87}\text{Rb}/^{86}\text{Sr}$  for the intrusive rock samples of the Never Summer igneous complex. Black and green lines represent 28 and 500 Ma reference isochrons, respectively. **a** Displays intrusive rocks rock samples with  $^{87}\text{Rb}/^{86}\text{Sr} < 300$ . **b** Focuses on samples with  $^{87}\text{Rb}/^{86}\text{Sr} < 10$

heterogeneous (wt%  $\text{SiO}_2$  from 54 to 67,  $\epsilon_{\text{Nd}}(\text{T})$  from  $-0.5$  to  $-5.7$ ). In contrast, all of the highly silicic intrusive rocks analyzed, including the syenogranites of the Mt. Cumulus stock ( $\sim 28.02$  Ma), have comparatively uniform chemical and isotopic compositions (wt%  $\text{SiO}_2 \sim 75$ ,  $\epsilon_{\text{Nd}}(\text{T}) \sim -5.6$ ). Our goal is to establish why these compositional differences exist and to assess what implications these differences have for understanding the continental magmatic system operating beneath the Never Summer region during the Oligocene.

#### Origin of the Mt. Cumulus stock: a product of anatexis of mafic, Precambrian lower continental crust

The Mt. Cumulus stock, the subsurface granite porphyries at Jack Creek (Fig. 1), and the late-stage silicic dike, all have major and trace element abundances similar to those observed in high-silica topaz rhyolites from the western USA (Christiansen et al. 2007). Topaz rhyolites have low eruptive temperatures ( $650$ – $700$  °C), generally low  $f\text{O}_2$ , and

a small, but definite range of wt%  $\text{SiO}_2$  compositions at and above  $\sim 75$  wt%. These rhyolites are ferroan and weakly peraluminous, have high LIL and HFSE abundances, and low  $\text{Rb}/\text{Nb}$  ( $< 3$ ). Their LREE and Sr abundances, and  $\text{Eu}^*/\text{Eu}$  negatively correlate with increasing wt%  $\text{SiO}_2$  (Christiansen et al. 2007). The silicic intrusive rocks in the Never Summer Mountains share these same chemical characteristics. Granite porphyries associated with Oligocene, Climax-type porphyry Mo deposits, in the Southern Rocky Mountains, including the Urad–Henderson deposit located only 30 km south of the Never Summer Mountains (Fig. 1), share similar chemical characteristics (Bookstrom et al. 1988). We conclude that the silicic intrusive rocks in the Never Summer Mountains are variants of granitic rocks associated with Climax-style porphyry Mo deposits found elsewhere in the region, and all are intrusive equivalents of topaz rhyolites.

In topaz rhyolites, decreasing Eu, Ba, and Sr abundances with increasing wt%  $\text{SiO}_2$  can be attributed to (alkali) feldspar fractionation, decreasing LREE abundance to the removal of a LREE accessory phase (e.g., chevkinite, allanite), decreasing Hf and Zr to the removal of zircon, and decreasing P contents to apatite fractionation (Christiansen et al. 2007). A similar interpretation can be applied to the chemical variations observed in the Never Summer igneous complex silicic intrusive rocks, which implies that these rocks also represent crystallized melt compositions. None of the intrusive rocks have Ba or Sr contents that might be interpreted as cumulate material, although we recognize that identifying cumulate related to high-silica rhyolites is not straightforward (Gelman et al. 2014). Furthermore, the apparent lack of inherited cores in zircon and the absence of obvious crustal xenocrysts and xenoliths in the granitic rocks argue against a major role of upper crustal assimilation in their generation.

The  $\epsilon_{\text{Nd}}(\text{T})$  isotopic compositions estimated for the magmas parental to the highly silicic intrusive rocks ( $\sim -5$  to  $-6$ ) are distinct from those expected for mafic magmas derived from the sublithospheric mantle ( $+8$ ; Hofmann 1997) and from those derived from the lithospheric mantle, as estimated from the isotopic compositions of mafic magmatism involved in the production of the Mt. Richthofen stock ( $-2$ ; see below). Rather than being derived from closed system differentiation of a mafic parental magma, open-system processes, likely involving preexisting, lower  $\epsilon_{\text{Nd}}$  continental crust, are required.

Christiansen et al. (2007) noted that topaz rhyolites elsewhere in the Rocky Mountain region and the eastern Great Basin have higher  $\epsilon_{\text{Nd}}$  values than local, felsic composition Precambrian crust and concluded that the magmas parental to these rhyolites were either derived from mafic Precambrian crust or a mixture of high  $\epsilon_{\text{Nd}}$  mafic magmas and intermediate to felsic Precambrian crust,

**Table 3** Isotopic analyses of the Mt. Richthofen stock, Mt. Cumulus stock, and associated rocks

Sample no.	Rb (ppm) <sup>a</sup>	Sr (ppm) <sup>a</sup>	$^{87}\text{Rb}/^{86}\text{Sr}$	$^{87}\text{Rb}/^{86}\text{Sr}$ unc	$^{87}\text{Sr}/^{86}\text{Sr}_{\text{(M)}}^{\text{c}}$	error	$^{87}\text{Sr}/^{86}\text{Sr}_{\text{(T)}}^{\text{b}}$	Sm (ppm) <sup>a</sup>	Nd (ppm) <sup>a</sup>	$^{147}\text{Sm}/^{144}\text{Nd}$	$^{143}\text{Nd}/^{144}\text{Nd}_{\text{(M)}}^{\text{d}}$
<i>Mt. Richthofen stock</i>											
10-KJ-MR-75C	134	516	0.750504	0.010614	0.708164	11	0.707711	8.99	52.1	0.104394	0.512363
10-KJ-MR-96	110	685	0.464088	0.006563	0.707729	13	0.707537	10.6	55.9	0.114723	0.512373
10-KJ-MR-97	130	673	0.558247	0.007895	0.709512	6	0.709266	10.8	60.1	0.108719	0.512342
10-KJ-MR-103	164	330	1.436242	0.020312	0.712515	9	0.711923	8.33	45.7	0.110277	0.512395
10-KJ-MR-107	78	716	0.314832	0.004452	0.708532	8	0.708402	8.99	52.5	0.103599	0.512385
10-KJ-MR-109	71	1025	0.200185	0.002831	0.704984	8	0.704901	12.8	71.6	0.108156	0.512594
10-KJ-MR-110	92	821	0.323849	0.004580	0.706400	17	0.706264	7.83	46.3	0.102314	0.512337
11-KJ-MR-111	90	906	0.287086	0.004060	0.705616	13	0.705500	6.17	38.2	0.097719	0.512324
07COMR-2	107	877	0.352600	0.004987	0.705933	17	0.705782	6.62	41.3	0.096976	0.512339
11-KJ-MR-115	130	622	0.604019	0.008542	0.708561	10	0.708314	10.4	57.8	0.108858	0.512366
10-KJ-MR-116	140	625	0.647360	0.009155	0.708510	9	0.708247	10.3	56	0.111277	0.512331
11-KJ-MR-120	78	1046	0.215507	0.003048	0.706931	6	0.706836	8.02	46	0.105480	0.512495
11-KJ-MR-123	125	882	0.409580	0.005792	0.709321	11	0.709121	10	54.1	0.111830	
11-KJ-MR-124	79	1067	0.213974	0.003026	0.705894	18	0.705795	9.7	52.6	0.111568	0.512518
11-KJ-MR-132	112	529	0.611871	0.008653	0.708827	11	0.708567	10.5	58.7	0.108220	0.512408
Enclave											
11-KJ-MR-122	146	652	0.647147	0.009152	0.706529	9	0.706258	13	70.1	0.112197	0.512512
<i>Mt. Cumulus stock</i>											
Surface samples											
10-KJ-MC-94	385	4	278.16	3.933812	0.800950	39		10.50	35.9	0.176950	0.512363
10-KJ-MC-91	382	3	367.99	5.204212	0.836558	32		10.90	41.5	0.158904	0.512345
10-KJ-MC-89	181	83	6.30	0.089128	0.712079	8		9.13	48.4	0.114125	0.512342
Core samples											
10-DC-521-2-912	272	2	393.04	5.558425	0.765955	15		14.00	44.5	0.190337	0.512341
10-DC-521-4-931	344	4	248.54	3.514886	0.816515	38		13.50	41.1	0.198723	0.512323
10-DC-521-4-1597	307	15	59.15	0.836488	0.743154	42		13.80	46.8	0.178397	0.512356
Dike											
10-KJ-MR-78	165	101	4.72	0.066769	0.711803	9		12.00	48.9	0.148466	0.512372
Sample no.	Error	$\epsilon_{\text{Nd}}^{\text{e}}$	$\mu^{\text{a}}$	$\kappa^{\text{a}}$	$^{208}\text{Pb}/^{204}\text{Pb}_{\text{(M)}}^{\text{f}}$	$^{207}\text{Pb}/^{204}\text{Pb}_{\text{(M)}}$	$^{206}\text{Pb}/^{204}\text{Pb}_{\text{(M)}}$	$^{208}\text{Pb}/^{204}\text{Pb}_{\text{(T)}}^{\text{b}}$	$^{207}\text{Pb}/^{204}\text{Pb}_{\text{(T)}}$	$^{206}\text{Pb}/^{204}\text{Pb}_{\text{(T)}}$	
<i>Mt. Richthofen stock</i>											
10-KJ-MR-75C	10	-5.02	11.27	5.53	38.229		15.507	18.233	38.142	15.506	18.183
10-KJ-MR-96	17	-4.87	10.82	4.64	38.251		15.515	18.240	38.181	15.514	18.192
10-KJ-MR-97	13	-5.45	8.67	5.02	38.486		15.515	18.295	38.425	15.514	18.257
10-KJ-MR-103	15	-4.42	12.98	4.77	38.726		15.555	18.579	38.640	15.554	18.522
10-KJ-MR-107	9	-4.59	8.29	4.64	38.215		15.513	18.232	38.161	15.512	18.195
10-KJ-MR-109	13	-0.53	8.05	4.44	38.154		15.519	18.172	38.104	15.518	18.137
10-KJ-MR-110	20	-5.52	8.61	5.03	37.786		15.469	17.757	37.725	15.468	17.719
11-KJ-MR-111	16	-5.76	11.25	4.76	37.575		15.451	17.654	37.500	15.450	17.605
07COMR-2	18	-5.47	13.83	5.09	37.924		15.476	17.970	37.826	15.475	17.909
11-KJ-MR-115	18	-4.98	11.71	4.30	38.689		15.540	18.429	38.619	15.539	18.378
10-KJ-MR-116	12	-5.67	10.63	4.84	38.290		15.531	18.334	38.218	15.530	18.287
11-KJ-MR-120	11	-2.45	4.94	4.79	38.224		15.505	18.169	38.191	15.504	18.147
11-KJ-MR-123			5.69	7.88	38.301		15.529	18.354	38.238	15.528	18.329
11-KJ-MR-124	13	-2.03	6.19	5.73	38.026		15.488	18.115	37.976	15.487	18.088
11-KJ-MR-132	12	-4.16	21.18	4.83	38.120		15.579	18.698	37.978	15.578	18.605
Enclave											
11-KJ-MR-122	14	-2.15	8.74	3.70	38.287		15.514	18.217	38.242	15.513	18.178

**Table 3** continued

Sample no.	Error	$\epsilon_{\text{Nd}}^{\text{e}}(\text{T})$	$\mu^{\text{a}}$	$\kappa^{\text{a}}$	$^{208}\text{Pb}/^{204}\text{Pb}_{\text{(M)}}^{\text{f}}$	$^{207}\text{Pb}/^{204}\text{Pb}_{\text{(M)}}$	$^{206}\text{Pb}/^{204}\text{Pb}_{\text{(M)}}$	$^{208}\text{Pb}/^{204}\text{Pb}_{\text{(T)}}^{\text{b}}$	$^{207}\text{Pb}/^{204}\text{Pb}_{\text{(T)}}$	$^{206}\text{Pb}/^{204}\text{Pb}_{\text{(T)}}$
<i>Mt. Cumulus stock</i>										
Surface samples										
10-KJ-MC-94	8	-5.29	13.76	10.05	38.619	15.508	18.267	38.427	15.507	18.207
10-KJ-MC-91	12	-5.58	25.63	4.37	38.741	15.523	18.301	38.585	15.522	18.189
10-KJ-MC-89	19	-5.47	25.27	3.39	38.724	15.530	18.294	38.605	15.529	18.184
Core samples										
10-DC-521-2-912	26	-5.77	25.95	2.69	38.807	15.548	18.474	38.710	15.547	18.361
10-DC-521-4-931	15	-6.15	42.22	2.58	38.803	15.545	18.507	38.651	15.543	18.323
10-DC-521-4-1597	16	-5.43	22.70	4.37	38.754	15.534	18.364	38.616	15.533	18.265
<i>Dike</i>										
10-KJ-MR-78	18	-5.02	14.05	4.01	38.830	15.580	18.683	38.751	15.579	18.621

<sup>a</sup> Concentration determinations for Rb, Sr, Sm, and Nd in addition to Pb, U, and Th, used to determine  $\mu$  and  $\kappa$  values, were done by ICP-MS as reported in Table 2

Total procedural blanks averaged ~1 ng for Sr and Pb, and 100 pg for Nd, during study period

<sup>b</sup> Initial ratios were calculated at 28 Ma

<sup>c</sup>  $^{87}\text{Sr}/^{86}\text{Sr}$  ratios were analyzed using four-collector static mode measurements. Errors are  $2\sigma$  of mean and refer to last two digits of the  $^{87}\text{Sr}/^{86}\text{Sr}$  ratio

Forty-five measurements of SRM-987 during the study period yielded mean  $^{87}\text{Sr}/^{86}\text{Sr} = 0.710279 \pm 10$  ( $2\sigma$  mean)

<sup>d</sup> Measured  $^{143}\text{Nd}/^{144}\text{Nd}$  were normalized to  $^{146}\text{Nd}/^{144}\text{Nd} = 0.7219$ . Analyses were dynamic mode, three-collector measurements. Errors are  $2\sigma$  of mean and refer to last two digits of the  $^{143}\text{Nd}/^{144}\text{Nd}$  ratio

Thirty-six measurements of the La Jolla Nd standard during the study period yielded a mean  $^{143}\text{Nd}/^{144}\text{Nd} = 0.511834 \pm 8$  ( $2\sigma$  mean)

<sup>e</sup>  $\epsilon_{\text{Nd}}$  values calculated using a present-day  $^{143}\text{Nd}/^{144}\text{Nd}$  (CHUR) = 0.512638

<sup>f</sup> Pb isotopic analyses were four-collector static mode measurements. Measured Pb isotope ratios were corrected to SRM-981 values ( $^{208}\text{Pb}/^{204}\text{Pb} = 36.721$ ,  $^{207}\text{Pb}/^{204}\text{Pb} = 15.491$ ,  $^{206}\text{Pb}/^{204}\text{Pb} = 16.937$ )

Fourteen measurements of SRM-981 during the study period yielded  $^{208}\text{Pb}/^{204}\text{Pb} = 36.534 \pm 0.203$ ,  $^{207}\text{Pb}/^{204}\text{Pb} = 15.440 \pm 0.067$ ,  $^{206}\text{Pb}/^{204}\text{Pb} = 16.898 \pm 0.050$  ( $2\sigma$  mean)

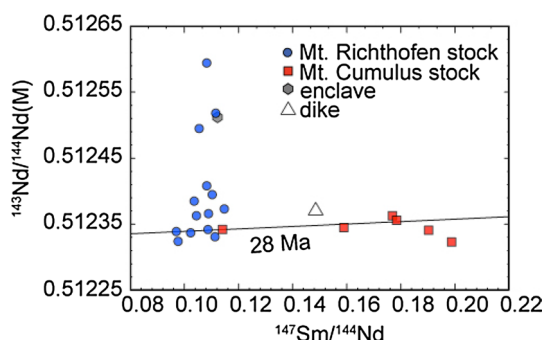


**Fig. 8** Measured  $^{143}\text{Nd}/^{144}\text{Nd}$  versus  $^{147}\text{Sm}/^{144}\text{Nd}$  for the intrusive rock samples of the Never Summer igneous complex. Black line represents a 28 Ma reference isochron

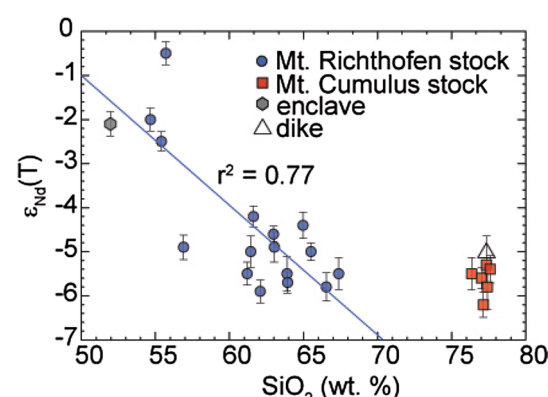


**Fig. 9** Plot of  $\text{SiO}_2$  versus  $\epsilon_{\text{Nd}}(\text{T})$  for the intrusive rock samples from the Never Summer igneous complex. Regression line is fitted to the Mt. Richthofen stock compositions

but not from high metamorphic grade felsic Precambrian crust, as argued for porphyry molybdenum-related granitic rocks in Colorado (Stein and Crock 1990). Christiansen et al. (2007) questioned Paleoproterozoic mafic crust as the sole source of these melts because this crust has significantly lower Fe/Mg and higher Rb/Nb than topaz rhyolites, at least where sampled as xenoliths in

Tertiary volcanic rocks that erupted along the southern margin of the Colorado Plateau. Instead, they favored a component in the topaz rhyolite magmas of intraplate (not subduction related) basalts, either as melt or as remobilized crystallized material within the continental crust.

In north-central Colorado, the role of crustal anatexis in the generation of silicic magmas can be more directly assessed using crustal xenoliths entrained in the nearby Devonian State Line kimberlites (Fig. 12). These xenoliths not only sample Precambrian crust in the vicinity of the Never Summer Mountains, but also provide a snapshot of the crustal composition prior to the onset of Late Cretaceous and younger magmatism in this region. The State Line xenoliths include two-pyroxene ( $\pm$  amphibole) granulites, two-pyroxene-garnet granulites, and cpx-garnet granulites (Bradley 1985) which demonstrate that the Devonian lower crust in this region was mafic in composition and dominated by garnet-bearing lithologies in its lowermost portions. Thermobarometry from the garnet-bearing xenoliths yields last equilibration pressures and temperatures of  $\sim$ 1.1 GPa and  $\sim$ 800 °C, which requires a Devonian crustal thickness of at least 35–40 km (Bradley 1985; Farmer et al. 2005). U–Pb ages from zircon present in mafic composition xenoliths range from  $\sim$ 1.6 to 1.73 Ga and overlap the ages of intermediate to felsic composition Paleoproterozoic crust exposed in this region (Farmer et al. 2005). The major and trace element abundances of the mafic xenoliths, although modified by interaction with the host kimberlites, further suggest that the crust was tholeiitic in composition and lacked prominent relative depletions in Nb and Ta on primitive mantle normalized trace element plots (Supplementary Material; Farmer et al. 2005). Much of this crust was moderately LREE enriched, although a few of these xenoliths have significantly lower  $(\text{La/Yb})_{\text{N}}$  (“N” meaning normalized to primitive mantle) ratios and may represent restites after partial lower crustal melting at 1.4 Ga (Farmer et al. 2005). Overall, the average composition of the lower crust beneath northern Colorado in the Devonian, estimated from the xenolith data (Supplementary Material), is consistent with that required for melts parental to topaz rhyolites (high Fe/Mg, low Rb/Nb; Christiansen et al. 2007). However, given the wide range of xenolith trace element abundances, including the wide range of xenolith Rb/Nb ratios (0.7–23; Farmer et al. 2005), it is not clear that the xenolith trace element data can be used to unequivocally fingerprint the source regions of the uniformly low Rb/Nb ( $\sim$ 3) silicic intrusive rocks in the Never Summer igneous complex.

It is also likely that this mafic crust was present and available for melting in the Oligocene. The Precambrian continental crust beneath north-central Colorado today is  $\sim$ 45 to 50 km thick, displays a 5–10 km thick  $\sim$ 7.2 km/s P-wave velocity layer (“7.xx” layer) at its base, and a clearly delineated Conrad discontinuity at  $\sim$ 20 km (Snelson et al. 2005). These observations suggest that, as in the Devonian, the present-day crust in north-central Colorado is mafic in composition below  $\sim$ 20 km and includes a thick,

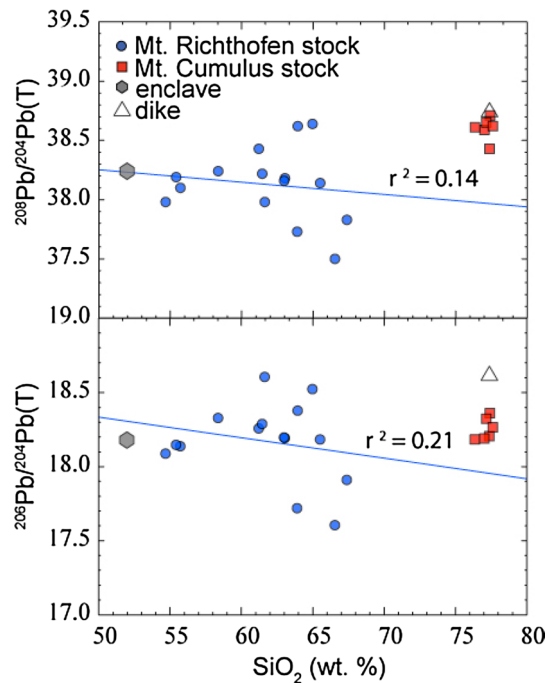


**Fig. 10** Plot of  $\text{SiO}_2$  versus  $^{208}\text{Pb}/^{204}\text{Pb}(\text{T})$  and  $^{206}\text{Pb}/^{204}\text{Pb}(\text{T})$  for the intrusive rock samples from the Never Summer igneous complex. Regression lines are fitted to the Mt. Richthofen stock compositions

garnet-bearing lowermost crust. As a result, mafic lower crust sampled by the State Line diatremes in the Devonian could remain intact today and so was likely available as a source of magmatism in the Oligocene.

Further supporting the possibility that the silicic igneous rocks in the Never Summer Mountains were derived from anatexis of mafic, Paleoproterozoic crust are the overlapping Nd isotopic compositions of both lithologies. In the mid-Tertiary, Paleoproterozoic crust in Colorado and vicinity plotted along an  $\sim$ 1.7 Ga reference Sm–Nd isochron, with felsic rocks having lower Sm/Nd ratios and lower  $\epsilon_{\text{Nd}}$  values than the mafic lower continental crust (Fig. 12). The  $\epsilon_{\text{Nd}}(28 \text{ Ma}) \sim -6$  for the Mt. Cumulus stock overlaps the values expected for mafic, not intermediate to felsic, crust (Fig. 12). The  $^{87}\text{Sr}/^{86}\text{Sr}(\text{T})$  of the Mt. Cumulus stock samples with the lowest  $^{87}\text{Rb}/^{86}\text{Sr}$ , our best estimates for the initial Sr isotopic compositions of their silicic parental magmas ( $\sim$ 0.710), also overlap the values determined for the “high  $(\text{La/Yb})_{\text{N}}$ ” mafic State Line xenoliths at 28 Ma (Farmer et al. 2005).

Overall, the available data are consistent with the derivation of the highly silicic igneous rocks in the Never Summer Mountains solely from mafic crustal anatexis, with no contribution of contemporaneous, mafic, mantle-derived magma. If so, then the abundances of garnet compatible elements (HREE, Y) in the silicic igneous rocks should

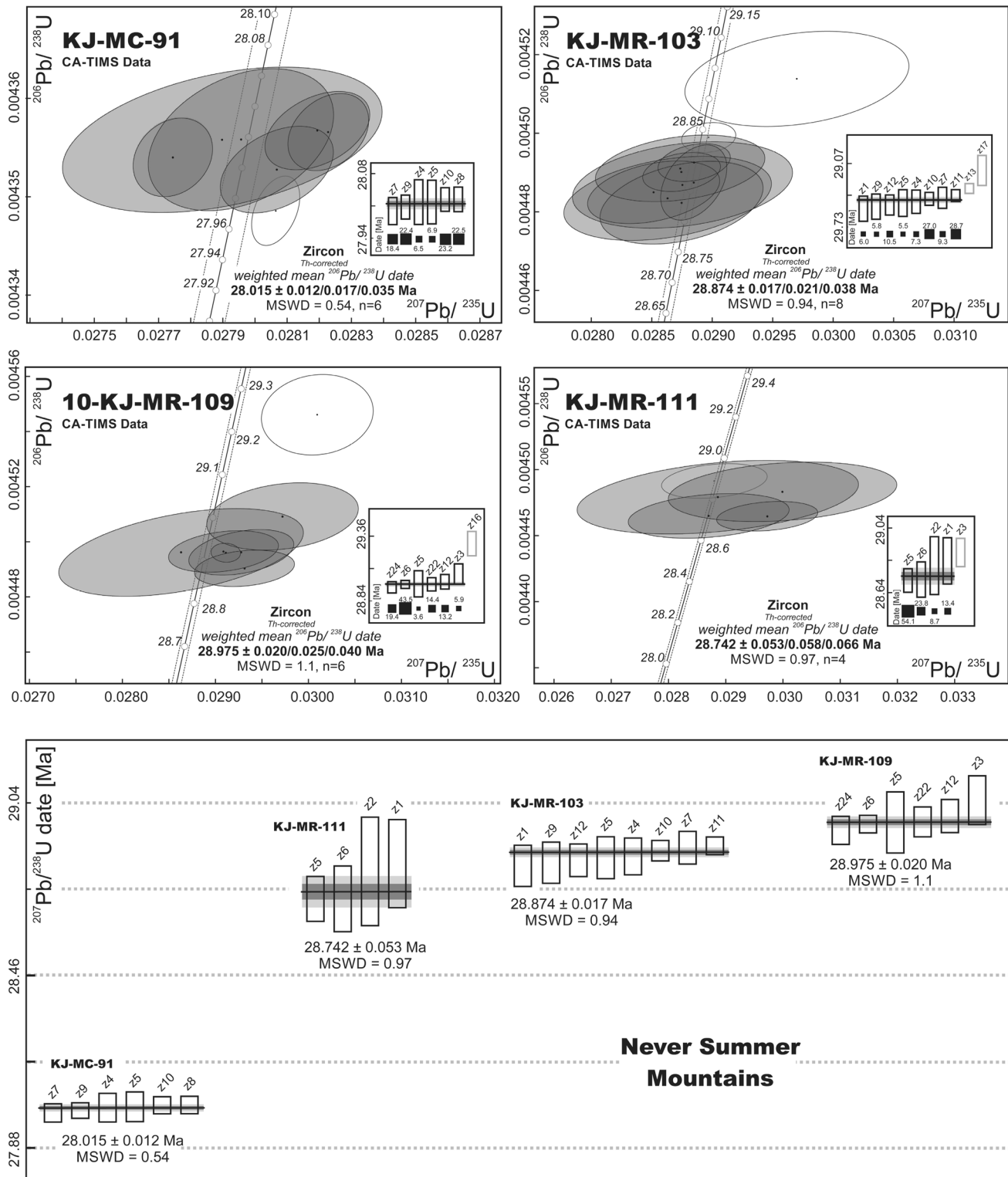


**Fig. 11** Conventional U–Pb Concordia diagram for zircon from the Mt. Cumulus and Mt. Richthofen stocks. Unshaded error ellipses indicate analyses excluded from the final age assignment. Age tick marks are labeled in millions of years along Concordia

provide evidence of whether the silicic melts were derived from the lowermost garnet-bearing lithologies, or shallower, garnet-absent (amphibole-bearing) mafic crust. To address

this question, we generated a set of estimated trace element abundances for 1 % partial batch melts of garnet-bearing and garnet-free State Line diatreme mafic xenoliths and

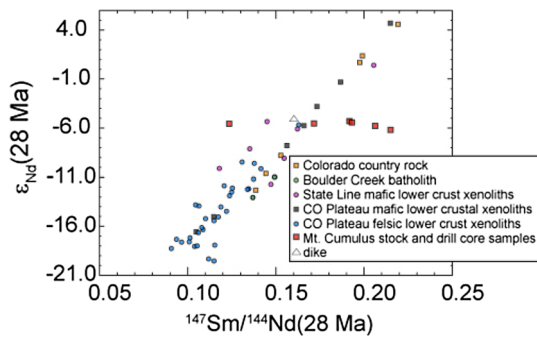


**Fig. 12** Whole rock Sm–Nd isochron for samples of the silicic intrusive rocks of the Never Summer igneous complex with data from other studies including Colorado country rocks, and lower- and mid-to upper crustal xenoliths from the Devonian State Line and Four Corners area diatremes. All  $\epsilon_{\text{Nd}}(\text{T})$  and  $^{147}\text{Sm}/^{144}\text{Nd}$  values are calculated at 28 Ma. Data from DePaolo (1981), Wendlandt et al. (1993), Condie et al. (1999), Farmer et al. (2005)

compared these abundances to those observed for the Never Summer Mountains area silicic intrusive rocks (Fig. 13). Rare earth element, Sr, and Y mineral-melt partition coefficients used were those estimated by Bédard (2006) and Nehring et al. (2009) for the anatexis of mafic granulites (see Supplementary Material). The average source rock trace element abundances used were those from the “high La/Yb<sub>N</sub>” State Line diatreme xenoliths (Farmer et al. 2005), and the range of mineral modes for these xenoliths were from Bradley (1985). As expected, partial melts of garnet-bearing lithologies produce much higher La/Yb, lower absolute HREE abundances, and higher Sr/Y than melts from garnet-absent mafic crust (Fig. 14). In the latter case, La/Yb ratios vary over a narrow range, with higher values being produced only for amphibole  $\pm$  clinopyroxene residual mineralogies (Fig. 14). All of the silicic igneous rocks have low Sr/Y, low La/Yb, and high HREE abundances expected from partial melting of garnet-absent rocks. This comparison, however, is complicated by the fact that none of the silicic rocks analyzed likely represent the primary melt produced by crustal anatexis. The covariations between increasing wt% SiO<sub>2</sub>, decreasing Sr/Y, decreasing La/Yb, and decreasing Eu/Eu\*, for example, likely represent progressive differentiation of a parental silicic melt through removal of feldspar and an LREE-enriched accessory mineral phase such as allanite or monazite (Fig. 14). However, the lowest wt% SiO<sub>2</sub>, least differentiated, parental silicic rocks have trace element ratios more similar to the values expected for primary melts of garnet-absent mafic crust. In fact, the trace element abundances of the highest wt% SiO<sub>2</sub> portion of the Mt. Richthofen stock, which could be an early manifestation of the silicic magmatism (see below), overlap the values expected for melting of amphibole-bearing,

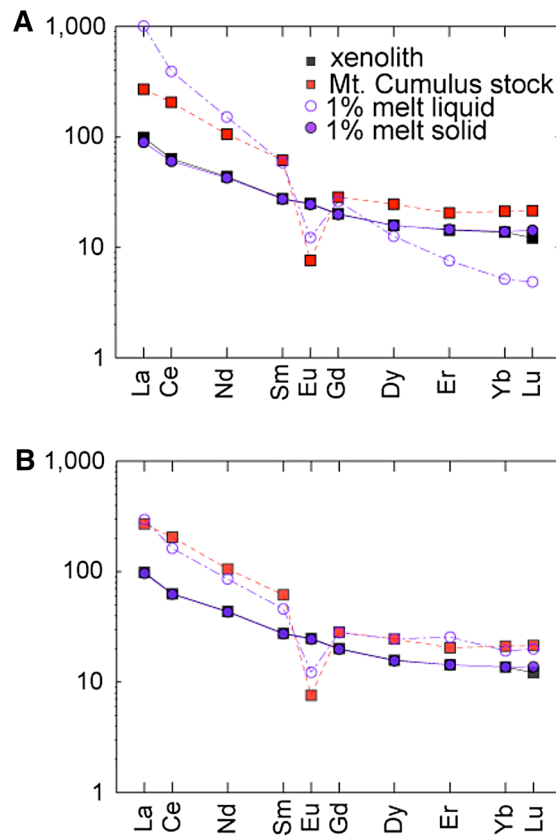


**Fig. 13** Rare earth element models showing the range of REE composition of a liquid and its residual solid after 1 % partial melting. Plotted for reference are the REE abundances of the sample from the Mt. Cumulus stock which contains the lowest wt% SiO<sub>2</sub> and an average of the REE abundances from high La/Yb<sub>N</sub> State Line diatreme xenoliths from Farmer et al. (2005). **a** Melting of a garnet-bearing two-pyroxene source with approximate modal compositions from Farmer (2005); 20.9 % plagioclase, 31 % orthopyroxene, 24 % clinopyroxene, 10.9 % garnet, 6 % amphibole, 0.1 % apatite. **b** Melting of a garnet-free two-pyroxene source with approximate modal compositions from Bradley (1985); 50 % plagioclase, 20 % orthopyroxene, 24 % clinopyroxene, 4 % amphibole, 2 % apatite

garnet-absent lithologies. These observations indicate that if the silicic melts are derived from anatexis of mafic Precambrian crust, this melting did not occur in the lowermost, garnet-bearing crust, but instead occurred in shallower (~30 to ~20 km), garnet-free crust. A garnet-free crustal source has also been proposed for the magmas parental to mid-Tertiary granite porphyries related to molybdenum mineralization in Colorado (Stein and Crock 1990).

As an aside, we point out that the highest silica rocks (>77 wt% SiO<sub>2</sub>) are likely the product of magmatic differentiation in the upper crust and do not represent the compositions of the original anatetic parental magmas (Gualda and Ghiorso 2013). If so, then the deep negative Eu anomalies observed in the silicic rocks must be the

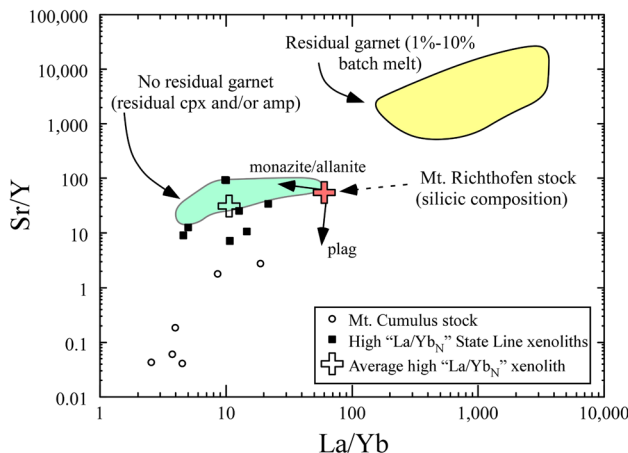


**Fig. 14** Sr/Y versus La/Yb for the Mt. Cumulus Stock, “high La/Yb” State Line xenoliths, and for modal batch melts (1–10 %) of various mafic granulites from State Line xenoliths (mineral modes from Bradley 1985). Partition coefficients for La and Yb from Nehring et al. (2010) for melting of mafic granulite. Sr and Y partition coefficients are for silicic melt compositions from Nash and Creecraft (1985), Sisson and Bacon (1992), Ewart and Griffin (1994), Hermann (2002), Prowatke and Klemme (2006), Bédard (2006), Stepanov et al. (2012)

product of alkali feldspar fractionation during shallow differentiation. This conclusion is consistent with the fact that even 10 % partial melting (not shown) of typical State Line two-pyroxene granulite xenoliths only generates melts with modest negative Eu anomalies ( $\text{Eu/Eu}^* \geq 0.9$ ) and leaves a residual solid with  $\text{Eu/Eu}^*$  of only 1.05–1.08, using mineral-melt partition coefficients from Nehring et al. (2009). Although high  $\text{Eu/Eu}^*$  feldspars must have accumulated somewhere within the crust, such a chemical signature was not likely imparted to the restite remaining after the original mafic lower crust melted.

#### A magma mixing origin for the Mt. Richthofen stock

The primary question with the Mt. Richthofen stock is the origin of its chemical and isotopic heterogeneity. The Sr, Nd, and Pb isotopic variations in the stock preclude any simple closed system mechanism for producing these heterogeneities, including basaltic magma underplating, reheating, and partial melting of an antecedent intermediate composition stock or crystal mush (Bachmann et al. 2007). Also, arguing for the importance of open-system processes in the formation of the Mt. Richthofen stock is the fact that the abundances of many major and trace elements vary linearly with increasing wt%  $\text{SiO}_2$ , the exceptions being elements such as Na and K (Fig. 4) that were likely remobilized during the low-T, post-solidification, epidote-chlorite alteration that affected the northern portions of the stock. Linear covariations on element

variation diagrams of intrusive igneous rocks are common and are generally interpreted as evidence of mixing (defined as the complete combination of two liquids) between mafic and felsic composition magmatic end-members (Sisson et al. 1996; Barnes et al. 2001; Slaby and Martin 2008), and we consider such an interpretation applicable to the Mt. Richthofen stock as well. In this scenario, the felsic magmatic end-member must have had chemical compositions at least as silicic as those determined for the western, more silicic, portions of the stock. Significantly, although the western portions of the Mt. Richthofen stock have lower wt%  $\text{SiO}_2$  than any of the younger, highly silicic intrusive rocks, all these rocks share similar initial Pb, Nd, and Sr isotopic compositions and similar incompatible trace element ratios (e.g., Rb/Nb at values of ~3). The Sr/Y and La/Yb ratios for the silicic portions of the stock are similar to the least siliceous of the younger silicic intrusive rocks (e.g., the late-stage dike) and are well within the range expected for anatetic melts of local, garnet-free mafic crust (Fig. 14). We suggest, then, that the silicic magmatic end-member involved in the production of the Mt. Richthofen stock was likely an undifferentiated version of the anatetic melts from which the younger silicic intrusive rocks crystallized.

The mafic end-member involved in magma mixing is more difficult to define. The mafic enclave swarms preserved along the eastern portions of the Mt. Richthofen stock (Fig. 2) certainly indicate that mafic magmas were present in the magma system and at least mingled (defined as the combination to two components where each component retains some of its identity) with more silicic material during magma generation and/or assembly of the stock. But there is no a priori reason to expect that these mingled mafic magmas were identical to mafic melts that efficiently intermixed with silicic magma to produce the bulk of the Mt. Richthofen stock. We note, however, that if our single enclave analysis is representative of the compositions of the entire enclave population, then the mingled magmas had chemical and isotopic compositions similar to the most mafic portions of the Mt. Richthofen stock. We recognize that the enclave compositions do not necessarily represent the composition of their original parental magmas due to diffusional exchange with their host rocks (Holden et al. 1991; Van der Laan and Wyllie 1993). Our intent is simply to suggest that enclave compositions indicate that mafic magmas with appropriate chemical and isotopic compositions were present during the construction of the Mt. Richthofen stock, lending credence to a mixing origin for its compositional characteristics. We also note that the Nd isotopic composition of the mafic enclave ( $\epsilon_{\text{Nd}} \sim -2$ ) is similar to Cenozoic basaltic rocks found elsewhere in the southern Rocky Mountain region ( $\epsilon_{\text{Nd}} \sim -2$  to 0) and all

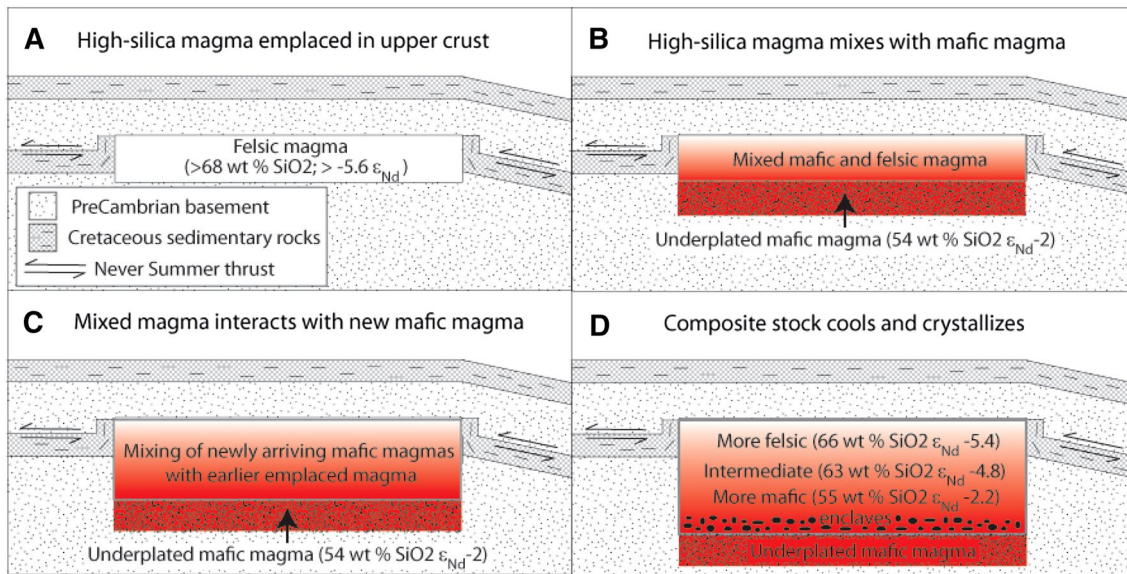


**Fig. 15** Schematic diagram of the in situ construction of the Mt. Richthofen stock. **a** A high-silica melt intrudes into the upper crust. **b** A later arriving batch of mafic magmas underplates and mixes with the high-silica melt. **c** The vertically zoned stock continues to

mix with subsequently arriving mafic magmas. **d** As the stock cools, newly arriving magmas mingle and quench, rather than mix with the stock to form mafic enclaves. *Note:* not drawn to scale

may represent mafic magmas derived from the lithospheric mantle (Bailley 2010).

Although a magma mixing origin for the Mt. Richthofen stock is consistent with the available data, it is not obvious whether mixing occurred in situ in the upper crust or at greater crustal depths. Complicating matters are the zircon U–Pb geochronology data, which reveal that the Mt. Richthofen stock does not ubiquitously yield the same date but instead appears to have been assembled over a time interval of  $\sim 230 \pm 53$  k.y., ending some  $727 \pm 54$  k.y. prior to the emplacement of the crosscutting Mt. Cumulus stock. The oldest zircon grains, presumably corresponding to the oldest portions of the stock, are from the eastern, more mafic rocks, while the youngest zircon grains are from the western, more silicic rocks. No obvious textural boundaries have been observed in the field to support this suggestion, but this may be due to the post-emplacement annealing of the boundaries between successively emplaced magma batches.

Given these observations, we consider two alternate possibilities for the construction of the Mt. Richthofen stock. The first is that the stock was constructed incrementally from silicic, anatetic melts that were emplaced in the upper crust ( $\sim 3$  km as estimated from hornblende geobarometry). The entire assembly was then melted and intermixed with underplated basaltic magma in situ (Fig. 15). The second possibility we consider is that mixing between silicic and mafic magmas occurred deeper in the crust, and that these mixed magmas were emplaced incrementally into the upper crust to construct the stock as a whole.

Basaltic underplating of antecedent, silicic intrusive rocks has been invoked to explain other hybrid igneous bodies including some in the eastern Sierra Nevada batholith in California (Coleman et al. 1995; Sisson et al. 1996; Wenner and Coleman 2004). Although an attractive option for the Mt. Richthofen stock, this process should have produced a vertical zonation in the stock from more mafic to more felsic compositions, a zonation that is not readily apparent from our data set. One issue is that any original spatial variation in the composition of the Mt. Richthofen stock could have been obscured by post-emplacement dissection of the stock along the north–south striking normal faults present on both the east and west flanks of the Never Summer Mountains (Fig. 1). However, a  $\sim 1$  km, east–west traverse through the central portion of the stock from Pinnacle Pool to west of the crest of the range is not obviously dissected by normal faults (Fig. 16) and provides an opportunity to determine whether any regular spatial compositional variations existed in the stock. From east to west along this transect, surface elevation and whole rock wt% SiO<sub>2</sub> increases and ε<sub>Nd(T)</sub> decreases (Fig. 16). This observation is consistent with the possibility that at least the eastern portions of the stock were zoned from mafic, higher ε<sub>Nd(T)</sub> compositions at its base to progressively more felsic, lower ε<sub>Nd(T)</sub> bulk compositions upwards. However, west of the mountain range crest, whole rock wt% SiO<sub>2</sub> does not vary regularly with elevation (Fig. 16). It is possible that the stock has experienced post-emplacement, down to the west tilting, along with down to the west normal faulting,

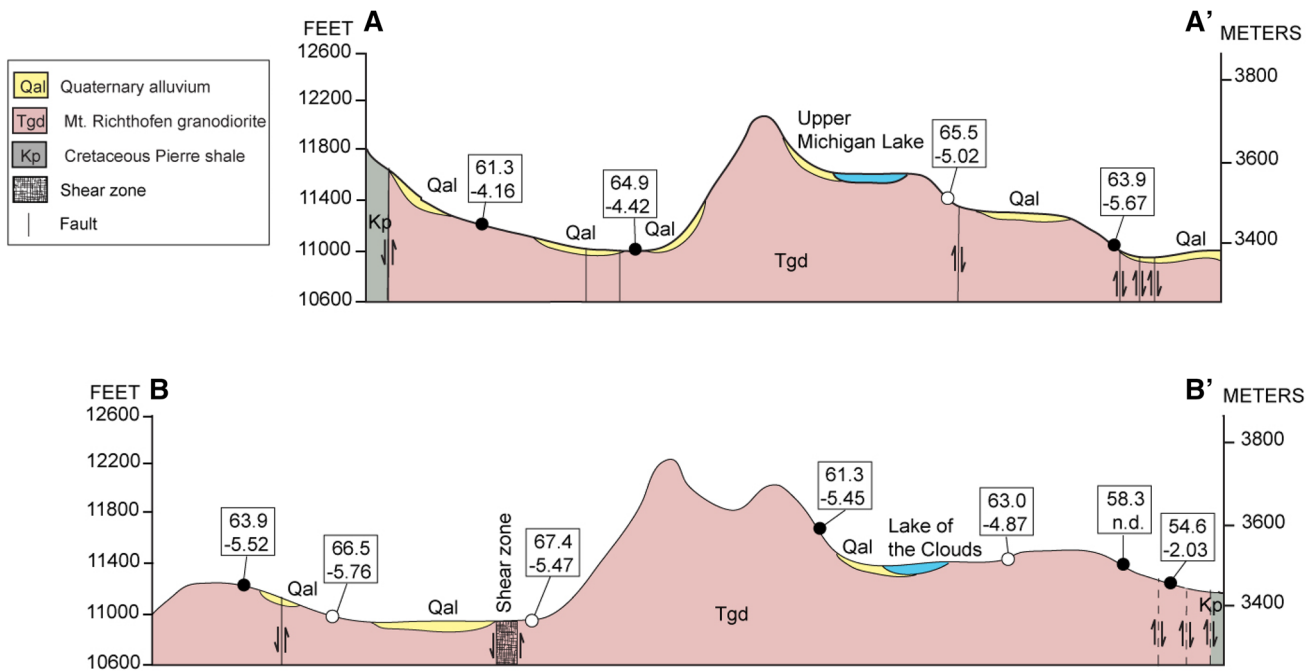


**Fig. 16** Cross section of the Mt. Richthofen stock with the  $\text{SiO}_2$  and  $\epsilon_{\text{Nd}}$  of select samples labeled along transects A–A' and B–B' (Fig. 1). Black circles were collected along the cross-sectional line. Open circles are projected in from closest sample location to cross-sectional line

both of which would bring the more silicic upper portions of the stock down to lower elevations. Tilting is well documented further south in the Front Range, in the vicinity of the Urad–Henderson porphyry molybdenum deposit (Fig. 1). However, tilting here is down to the east, not west, by  $\sim 20^\circ$  (Geissman et al. 1992; Kelley and Chapin 2004), which requires a shift in tilting direction north of the Urad–Henderson area along an ~E–W directed accommodation zone that has not yet been documented in the field. A simpler option is that the western portion of the stock is, in fact, a separate intrusive rock that was emplaced after the more mafic, eastern portions of the stock, as the U–Pb zircon geochronology data suggest.

Another issue is whether an antecedent silicic body could be heated above the granite solidus, via basaltic magma underplating, allowing for the possibility that in situ mixing of the two compositions could occur, given that the lifespan of this system was  $>1$  m yr. We consider a 1D instantaneous heating model to test whether the timescales required to heat a silicic, proto-Mt. Richthofen stock above the granite solidus (taken to be 750 °C) would be plausible given that the estimated lifetime of this system was likely  $\leq 1$  million years (Knox 2005). Our model assumes that the Mt. Richthofen stock was intruded as a 1-km-thick sill (Fig. 15) into the shallow crust at a maximum depth of 3 km. In our model, the 1-km-thick silicic composition sill intrudes into the upper crust, is allowed

to cool to country rock temperatures, and is then instantaneously heated from below by the emplacement of a continuously refreshed basalt source at 1200 °C. Temperatures above the granite solidus are achieved throughout the entire 1-km-thick sill in 60 k.y. and in just 15 k.y. temperatures above the granite solidus are achieved throughout half the sill ( $\kappa = 10^{-6} \text{ m}^2 \text{ s}^{-1}$ ). This simple model demonstrates that an antecedent, highly silicic body could have been brought to temperatures above the granite solidus well within the lifetime of this magma system by basaltic magma underplating, although it is not clear that the conditions produced were sufficient to provoke the efficient mixing that led to the production of the bulk of the Mt. Richthofen stock. A waning flux of mafic magma into the base of this system would have resulted in sufficient cooling of the stock so that the last underplated magmas mingled, rather than mixed with the base of the hybrid stock and were preserved as discrete phases.

The second possibility we consider is that mixing between silicic and mafic magmas occurred at depth in the crust, and that these magmas were emplaced incrementally in the upper crust to form a composite. This model is consistent with our U–Pb zircon geochronology data if the most mafic magma batches, containing the largest fraction of intermixed mafic magma, were intruded first and were followed by younger, more silicic magmas. This option neither requires or precludes underplating of the composite

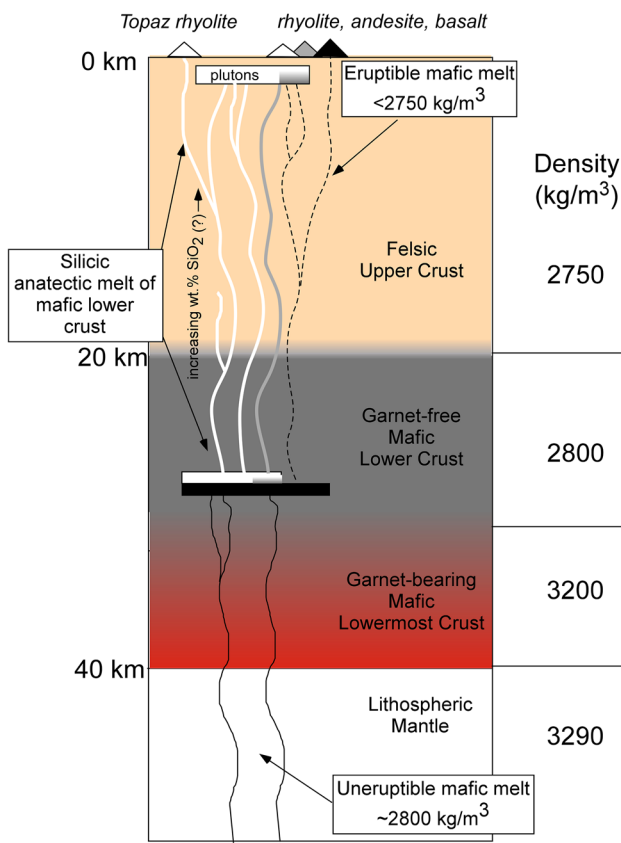


**Fig. 17** Schematic diagram of continental magma system supporting Never Summer igneous complex. Estimated crustal densities from Farmer et al. (2005) and Snelson et al. (2005)

stock by mafic magmas in the upper crust, although the lack of flattening or other flow induced lineations in the mafic enclaves (Fig. 2) seems more consistent with their emplacement *in situ* in the upper crust.

#### Reconstructing a small-volume continental magmatic system

The intrusive igneous rocks at the Never Summer igneous complex provide a record of the various magma types that were delivered to the upper continental crust in this region during the Oligocene and provide insights into how these magmas or their crystallized equivalents interacted. We contend that this record is decipherable largely because this magma system was small volume and short lived, leaving the processes involved in the production of specific igneous rocks relatively unobscured by repeated magmatic events. As a result, the Mt. Richthofen and Mt. Cumulus stocks retain evidence that reveals that magmas associated with the Never Summer igneous complex were fundamentally bimodal in composition. Silicic melts produced by anatexis

of garnet-free mafic lower continental crust were supplied to the upper crust throughout much of the magmatic episode. Interaction between silicic and mafic magmas, either *in situ* in the upper few kilometers of the crust or at deeper crustal levels, produced the spectrum of intermediate composition magmas from which much of Mt. Richthofen stock was constructed. Regardless of where mixing took place, the occurrence of mafic magmas in the upper crust supports the assertion that the Never Summer igneous complex was fueled by a mantle-melting event which resulted in the infiltration of basaltic magmas into the continental crust.

Why did mafic lower crustal anatexis occur in the Oligocene, and why was this anatexis isolated to the upper, garnet-free, portions of the lower crust? Several authors have suggested that the magmas parental to both topaz rhyolites and syenogranites related to molybdenum mineralization in the Rocky Mountain region were related to episodes of lithospheric extension (Stein and Hannah 1985; Ludington and Plumlee 2009). The fact that the Never Summer igneous complex was related to bimodal magmatism is consistent with this interpretation (Christiansen and McCurry 2008) despite available field evidence that Cenozoic extension in this region was small in magnitude and occurred post-28 Ma (Chapin and Cather 1994). Even if extension and crustal exhumation accompanied magmatism at the Never Summer igneous complex, exhumation alone cannot trigger dehydration melting of amphibolite in the lower crust without the addition of heat, presumably through the incursion of mantle-derived magmas (Thompson and Connolly 1995). The fact that mafic magmas were a part of the magma system related to the Never Summer intrusive rocks allows the possibility that lower crustal anatexis was related to the pooling of mafic magmas in the upper, garnet-free, portions of the lower crust, in a lower crustal “hot zone” (Annen 2006). We note that vapor-absent, dehydration melting of the lower crust is required, if the silicic intrusive rocks in the Never Summer region are truly the products of deep crustal anatexis, because water saturated silicic melts cannot ascend from <20 km depths to the surface without solidification (Holland and Powell 2001).

We can only speculate as to why the mafic magmas pooled in the upper portions of the lower crust. One possibility is that the ascent depth of mafic magmas was controlled by lower crustal density variations (Fig. 17). Bulk rock densities of the garnet-bearing lowermost crust in north-central Colorado, as directly determined from the State Line diatremes, are high (3,000–3,300 kg/m<sup>3</sup>) compared to those of shallower, two-pyroxene granulites (~2,700 to 2,800 kg/m<sup>3</sup>; (Farmer et al. 2005). Basaltic magmas in the lower crust likely have densities from ~3,000 to ~2,600 kg/m<sup>3</sup> depending on dissolved H<sub>2</sub>O and/or CO<sub>2</sub> contents (Lange 2002). As a result, it is possible that during

the Oligocene, mantle-derived basaltic melts ascended rapidly through the dense lower crust and pooled at a level of neutral buoyancy in the upper, garnet-free lower crust, triggering crustal anatexis (Fig. 17). If the volume of mafic magmas was sufficient, mixing between the basaltic magma and silicic anatexic melts could have occurred in situ in the lower crust, producing the intermediate composition magmas that ultimately reached the upper crust (Annen 2006). Differentiation of basaltic melts in the lower crust could also have occurred, producing lower density mafic magmas that ascended into the upper crust (Stolper and Walker 1980) and underplated earlier emplaced silicic intrusive rocks.

## Conclusions

Oligocene intrusive igneous rocks at the Never Summer igneous complex retain evidence of the igneous processes that occurred in the upper reaches of this small-volume continental magma system, processes that can be masked in larger volume systems. Our data demonstrate that magmatism in this system was bimodal with anatexic silicic melts and lithospheric mantle-derived mafic magmas being delivered to the upper crust. The highly silicic melts solidified to produce epizonal, syenogranites, or erupted as topaz rhyolites. Hybridization of an antecedent silicic igneous body and underplated mafic magmas, or injection of mixed magmas into the upper crust, resulted in the construction of the chemically and isotopically zoned Mt. Richthofen stock. No evidence exists at this igneous center that any silicic magmas were produced by partial melting of an antecedent, more mafic igneous body or crystal mush. We emphasize that the sequence of events outlined here represent processes involved in the evolution of the upper reaches of a small-volume system. These processes may also represent the incipient stages of evolution of larger magmatic systems or may be restricted to small-volume systems and completely bypassed in systems where volumes of melt present in a given crustal column are significantly larger.

**Acknowledgments** Support for this study was provided by The Geological Society of America, the Colorado Scientific Society, Rocky Mountain Association of Geologists, and the University of Colorado Department of Geological Sciences. The manuscript was greatly improved in response to reviews by Eric Christiansen and Calvin Miller. We thank Timothy L. Grove for his handling of the paper as executive editor. Laboratory assistance from Emily Verplanck was extremely helpful. We thank Judy Visty at Rocky Mountain National Park for granting us access to the Grand Ditch Road which made the remote Never Summer Mountains readily accessible. Electron microprobe work was carried out with the help of Julian Allaz at the University of Colorado. U–Pb geochronology carried out at MIT was made possible by NSF EAR-0931839.

## References

- Acosta-Vigil A, Buick I, Hermann J et al (2010) Mechanisms of crustal anatexis: a geochemical study of partially melted metapelite enclaves and Host Dacite, SE Spain. *J Petrol* 51:785–821. doi:[10.1093/petrology/egp095](https://doi.org/10.1093/petrology/egp095)
- Anderson J, Smith D (1995) The effects of temperature and  $fO_2$  on the Al-in-hornblende barometer. *Am Miner* 80:549–559
- Annen C (2006) The genesis of intermediate and silicic magmas in deep crustal hot zones. *J Petrol* 47:505–539. doi:[10.1093/petrology/egi084](https://doi.org/10.1093/petrology/egi084)
- Armstrong R, Ward P (1991) Evolving geographic patterns of cenozoic magmatism: the temporal and spatial association of magmatism and metamorphic core complexes. *J Geophys Res* 96:13201–13224
- Bachmann O, Miller CF, de Silva SL (2007) The volcanic–plutonic connection as a stage for understanding crustal magmatism. *J Volcan Geotherm Res* 167:1–23. doi:[10.1016/j.jvolgeores.2007.08.002](https://doi.org/10.1016/j.jvolgeores.2007.08.002)
- Bailley TL (2010) A reevaluation of the origin of late Cretaceous and younger magmatism in the southern Rocky Mountain region using space-time-composition patterns in volcanic rocks and geochemical studies of mantle xenoliths. PhD Thesis: University of Colorado, Boulder, p 166
- Barnes C, Burton B, Burling T (2001) Petrology and geochemistry of the late Eocene Harrison Pass pluton, Ruby Mountains core complex, northeastern Nevada. *J Petrol* 42:901–929
- Bédard JH (2006) A catalytic delamination-driven model for coupled genesis of Archaean crust and sub-continental lithospheric mantle. *Geochim Cosmochim Acta* 70:1188–1214. doi:[10.1016/j.gca.2005.11.008](https://doi.org/10.1016/j.gca.2005.11.008)
- Blundy JD, Holland TJB (1990) Calcic amphibole equilibria and a new amphibole–plagioclase geothermometer. *Contrib Miner Petrol* 104:208–224
- Bookstrom AA, Carten RB, Shannon JR, Smith RP (1988) Origins of bimodal leucogranite-lamprophyre suites, climax and Red Mountain Porphyry Molybdenum Systems, Colorado—petrologic and strontium isotopic evidence. *Color Sch Mines Q* 83:1–24
- Bradley S (1985) Granulite facies and related xenoliths from Colorado-Wyoming kimberlites. MSc Thesis: Colorado State University, pp 1–148
- Burgess SD, Bowring S, Shen Sz (2013) High-precision timeline for Earth's most severe extinction. *Proc Natl Acad Sci* 111:3316–3321. doi:[10.1073/pnas.1317692111](https://doi.org/10.1073/pnas.1317692111)
- Chapin CE, Cather SM (1994) Tectonic setting of the axial basins of the northern and central Rio Grande rift. In: Keller GR, Cather SM (eds) Basins Rio Gd. Rift Struct. Stratigr. Tecton. Setting, vol 291. Geological Society of America, Boulder, pp 5–26
- Christiansen EH, McCurry M (2008) Contrasting origins of Cenozoic silicic volcanic rocks from the western Cordillera of the United States. *Bull Volcan* 70:251–267. doi:[10.1007/s00445-007-0138-1](https://doi.org/10.1007/s00445-007-0138-1)
- Christiansen EH, Burt DM, Sheridan MF, Wilson RT (1983) The petrogenesis of topaz rhyolites from the western United States. *Contrib Miner Petrol* 83:16–30. doi:[10.1007/BF00373075](https://doi.org/10.1007/BF00373075)
- Christiansen E, Haapala I, Hart G (2007) Are Cenozoic topaz rhyolites the erupted equivalents of Proterozoic rapakivi granites? Examples from the western United States and Finland. *Lithos* 97:219–246. doi:[10.1016/j.lithos.2007.01.010](https://doi.org/10.1016/j.lithos.2007.01.010)
- Claiborne LL, Miller CF, Walker BA et al (2006) Tracking magmatic processes through Zr/Hf ratios in rocks and Hf and Ti zoning in zircons: an example from the Spirit Mountain batholith, Nevada. *Miner Mag* 70:517–543. doi:[10.1180/0026461067050348](https://doi.org/10.1180/0026461067050348)
- Cole JC, Larson E, Farmer L et al (2008) The search for Braddock's Caldera - Guidebook for Colorado Scientific Society fall 2008

- field trip, Never Summer Mountains, Colorado: US Geological Survey Open-File Report 2008-1360, pp 1–30
- Cole JC, Braddock WA (2009) Geologic map of the Estes Park 30' x 60' quadrangle, north-central Colorado: US Geological Survey Scientific Investigations Map 3039, scale 1:100,000, p 56
- Coleman DS, Glazner AF, Miller JS et al (1995) Exposure of a Late Cretaceous layered mafic-felsic magma system in the central Sierra Nevada batholith, California. *Contrib Miner Petrol* 120:129–136. doi:[10.1007/BF00287110](https://doi.org/10.1007/BF00287110)
- Condie K, Latysh N, Van Schmus W et al (1999) Geochemistry, Nd and Sr isotopes, and U-Pb Zircon ages of Granitoid and Metasedimentary Xenoliths from the Navajo Volcanic Field, Four Corners area, Southwestern United States. *Chem Geol* 156:95–133
- Coney PJ, Reynolds S (1977) Cordilleran Benioff zones. *Nature* 270:403–406
- DePaolo D (1981) Neodymium isotopes in the Colorado Front Range and crust-mantle evolution in the Proterozoic. *Nature* 291:193–196
- Ewart A, Griffin WL (1994) Application of proton-microprobe data to trace-element partitioning in Volcanic-rocks. *Chem Geol* 117:251–284
- Farmer GL, Broxton DE, Warren RG, Pickthorn W (1991) Nd, Sr, and O isotopic variations in metaluminous ash-flow tuffs and related volcanic rocks at the Timber Mountain/Oasis Valley Caldera, Complex, SW Nevada: Implications for the origin and evolution of large-volume silicic magma bodies. *Contrib Miner Petrol* 109:53–68
- Farmer GL, Bowring S, Williams M et al (2005) Constraining lower crustal evolution across an archean-proterozoic suture: physical, chemical and geochronological studies of lower Crustal Xenoliths in Southern Wyoming and Northern Colorado. In: Karlstrom KE, Keller RG (eds) The Rocky Mountain region: an evolving lithosphere, AGU Monograph, vol 154, pp 139–162
- Frost BR, Frost CD (2008) A geochemical classification for feldspathic igneous rocks. *J Petrol* 49:1955–1969. doi:[10.1093/petrology/egn054](https://doi.org/10.1093/petrology/egn054)
- Frost BR, Barnes C, Collins WJ et al (2001) A geochemical classification for granitic rocks. *J Petrol* 42:2033–2048. doi:[10.1093/petrology/42.11.2033](https://doi.org/10.1093/petrology/42.11.2033)
- Gamble BM (1979) Petrography and petrology of the Mt. Cumulus stock, Never Summer Mountains, Colorado. MSc Thesis: University of Colorado at Boulder, p 75
- Geissman J, Snee L, Graaskamp G et al (1992) Deformation and age of the Red Mountain intrusive system (Urad-Henderson molybdenum deposits), Colorado: evidence from paleomagnetic and  $^{40}\text{Ar}/^{39}\text{Ar}$  data. *Geol Soc Am Bull* 104:1031–1047. doi:[10.1130/0016-7606\(1992\)104<1031](https://doi.org/10.1130/0016-7606(1992)104<1031)
- Gelman SE, Bachmann O, Deering CD et al (2014) Identifying crystal graveyards remaining after large silicic eruptions. *Earth Planet Sci Lett* 393:266–274
- Glazner AF, Coleman DS, Bartley JM (2008) The tenuous connection between high-silica rhyolites and granodiorite plutons. *Geology* 36:183. doi:[10.1130/G24496A.1](https://doi.org/10.1130/G24496A.1)
- Gualda GAR, Ghiurso MS (2013) Low-pressure origin of high-silica rhyolites and granites. *J Geol* 121:537–545. doi:[10.1086/671395](https://doi.org/10.1086/671395)
- Harper BE, Miller CF, Koteas GC et al (2004) Granites, dynamic magma chamber processes and pluton construction: the Aztec Wash. *Trans R Soc Edinb Earth Sci* 95:277–295
- Hermann J (2002) Allanite: thorium and light rare earth element carrier in subducted crust. *Chem Geol* 192:289–330
- Hofmann AW (1997) Mantle geochemistry: the message from oceanic magmatism. *Nature* 385:219–229
- Holden P, Halliday AN, Stephens WE, Henney PJ (1991) Chemical and isotopic evidence for major mass transfer between mafic enclaves and felsic magma. *Chem Geol* 92:135–152
- Holland T, Blundy J (1994) Non-ideal interactions in calcic amphiboles and their bearing on amphibole-plagioclase thermometry. *Contrib Miner Petrol* 116:433–447. doi:[10.1007/BF00310910](https://doi.org/10.1007/BF00310910)
- Holland T, Powell R (2001) Calculation of phase relations involving haplogranitic melts using an internally consistent thermodynamic dataset. *J Petrol* 42:673–683
- Kelley S, Chapin C (2004) Denudation history and internal structure of the Front Range and Wet Mountains, Colorado, based on apatite-fission-track thermochronology. *N M Bur Geol Miner Resour* 160:41–77
- Kellogg KS (1999) Neogene basins of the northern Rio Grande rift: partitioning and asymmetry inherited from Laramide and older uplifts. *Tectonophysics* 305:141–152. doi:[10.1016/S0040-1951\(99\)00013-X](https://doi.org/10.1016/S0040-1951(99)00013-X)
- Knox K (2005) The Never Summer igneous complex. MSc Thesis: University of Colorado, pp 1–58
- Lange RA (2002) Constraints on the preeruptive volatile concentrations in the Columbia River flood basalts. *Geology* 30:179–182
- Leake B (1997) Nomenclature of amphiboles. *Can Miner* 61:295–321
- Lipman PW (2007) Incremental assembly and prolonged consolidation of Cordilleran magma chambers: evidence from the Southern Rocky Mountain volcanic field. *Geosphere* 3:42. doi:[10.1130/GES00061.1](https://doi.org/10.1130/GES00061.1)
- Ludington S, Plumlee G (2009) Climax-type porphyry molybdenum deposits. *US Geol Surv Open File Rep* 2009-1215:1–16
- McBirney A, Taylor H, Armstrong R (1987) Paricutin re-examined: a classic example of crustal assimilation in calc-alkaline magma. *Contrib Miner Petrol* 95:4–20
- McDonough WF, Sun S (1995) The composition of the Earth. *Chem Geol* 120:223–253
- Nash WP, Crecraft HR (1985) Partition-coefficients for trace-elements in silicic magmas. *Geochim Cosmochim Acta* 49:2309–2322
- Nehring F, Foley SF, Hölttä P (2009) Trace element partitioning in the granulite facies. *Contrib Miner Petrol* 159:493–519. doi:[10.1007/s00410-009-0437-y](https://doi.org/10.1007/s00410-009-0437-y)
- O'Neill JM (1976) The geology of the Mt. Richthofen Quadrangle and adjacent Kawuneeche Valley, North-central Colorado. PhD Thesis: University of Colorado, p 178
- O'Neill JM (1981) Geologic map of the Mt. Richthofen Quadrangle and the western part of the Fall River Pass Quadrangle, Grand and Jackson Counties, Colorado
- Prowatke S, Klemme S (2006) Trace element partitioning between apatite and silicate melts. *Geochim Cosmochim Acta* 70:4513–4527
- Putirka KD (2008) Thermometers and barometers for Volcanic systems. *Rev Miner Geochem* 69:61–120. doi:[10.2138/rmg.2008.69.3](https://doi.org/10.2138/rmg.2008.69.3)
- Sisson TW, Bacon CR (1992) Garnet high-silica rhyolite trace-element partition-coefficients measured by ion microprobe. *Geochim Cosmochim Acta* 56:2133–2136
- Sisson TW, Grove TL, Coleman DS (1996) Hornblende gabbro sill complex at Onion Valley, California, and a mixing origin for the Sierra Nevada batholith. *Contrib Miner Petrol* 126:81–108. doi:[10.1007/s004100050237](https://doi.org/10.1007/s004100050237)
- Slaby E, Martin H (2008) Mafic and felsic magma interaction in granites: the Hercynian Karkonosze Pluton (Sudetes, Bohemian Massif). *J Petrol* 49:353–391. doi:[10.1093/petrology/egm085](https://doi.org/10.1093/petrology/egm085)
- Nelson CM, Keller GR, Miller KC et al (2005) Regional crustal structure derived from the CD-ROM 99 seismic refraction/wide-angle reflection profile: the lower crust and upper mantle: Rocky Mountain region. *An Evol Lithosph* 154:271–291
- Stein HJ, Crock JG (1990) Late Cretaceous-Tertiary magmatism in the Colorado Mineral Belt: rare earth element and samarium-neodymium isotopic studies. In: Anderson JL (ed) Nat. Orig. Cordilleran Magmat, vol 174. *Geol. Soc. Am.*, Boulder, p 19

- Stein HJ, Hannah JL (1985) Movement and origin of ore fluids in clino-max-type systems. *Geology* 13:469–474
- Stepanov AS, Hermann J, Rubatto D, Rapp RP (2012) Experimental study of monazite/melt partitioning with implications for the REE, Th and U geochemistry of crustal rocks. *Chem Geol* 300:200–220
- Stolper E, Walker D (1980) Melt density and the average composition of Basalt. *Contrib Miner Petrol* 74:7–12
- Streckeisen A (1978) Classification and nomenclature of plutonic rocks. Recommendations of the IUGS subcommission on the systematics of igneous rocks. *Geol Rundschau Int Zeitschrift für Geol Stuttgart* 63:773–785
- Thompson AB, Connolly JAD (1995) Melting of the continental-crust—some thermal and petrological constraints on anatexis in continental collision zones and other tectonic settings. *J Geophys Res Earth* 100:15565–15579
- Van der Laan SR, Wyllie PJ (1993) Experimental interaction of granitic and basaltic magmas and implications for mafic enclaves. *J Petrol* 34:491–517
- Wendlandt E, Depaolo D, Baldridge W (1993) Nd and Sr isotope chronostratigraphy of Colorado Plateau lithosphere: implications for magmatic and tectonic underplating of the continental crust. *Earth Planet Sci Lett* 116:23–43
- Wenner JM, Coleman DS (2004) Magma mixing and cretaceous crustal growth: geology and geochemistry of granites in the Central Sierra Nevada Batholith, California magma mixing and cretaceous crustal growth: geology and geochemistry of granites in the Central Sierra Nevada Batholith. *Int Geol Rev* 46:880–903
- Wiebe R, Blair K, Hawkins D, Sabine C (2002) Mafic injections, in situ hybridization, and crystal accumulation in the Pyramid Peak granite, California. *Geol Soc Am Bull* 114:909–920. doi:[10.1130/0016-7606\(2002\)114<0909](https://doi.org/10.1130/0016-7606(2002)114<0909)